(12) INTERNATIONAL APPLICATION PUBLISHED UNDER THE PATENT COOPERATION TREATY (PCT)

(19) World Intellectual Property Organization
International Bureau

(43) International Publication Date
25 March 2010 (25.03.2010)

PCT

(10) International Publication Number
WO 2010/033267 A2

(51) International Patent Classification: Not classified

(21) International Application Number:
PCT/US2009/042966

(22) International Filing Date:
6 May 2009 (06.05.2009)

(25) Filing Language: English

(26) Publication Language: English

(30) Priority Data:
61/050,645 6 May 2008 (06.05.2008) US

(71) Applicant *(for all designated States except US)*: **UNIVERSITY OF GEORGIA RESEARCH FOUNDATION, INC.** [US/US]; 624 Boyd Graduate Studies Research Center, Athens, GA 30602-7411 (US).

(72) Inventors; and

(75) Inventors/Applicants *(for US only)*: **ZHAO, Yiping** [CN/US]; 1140 Harrowford Drive North, Statham, GA 30666 (US). **TRIPP, Ralph, A.** [US/US]; 1981 Oliver Bridge Rd., Watkinsville, GA 30677 (US). **DLUHY, Richard, A.** [US/US]; 165 Ravenwood Run, Athens, GA 30605 (US). **DRISKELL, Jeremy** [US/US]; 109 Woodhurst Dr., Athens, GA 30605 (US). **BOTTOMLEY, Lawrence** [US/US]; 3361 Connemara Trace, Lawrenceville, GA 30044 (US). **BARBER, Jabulani** [US/US]; 4505 Cahuengo Court, Fair Oaks, CA 95628 (US). **MAROTTA, Nicole** [US/US]; 771 Lindberg Dr., Apt. 5107, Atlanta, GA 30324 (US). **ABELL, Justin** [US/US]; 586 Franklin St., Athens, GA 30601 (US).

(74) Agent: **RHODEN, Melissa**; Thomas, Kayden, Horstemeyer & Risley, LLP, 600 Galleria Parkway, Suite 1500, Atlanta, GA 30339 (US).

(81) Designated States *(unless otherwise indicated, for every kind of national protection available)*: AE, AG, AL, AM, AO, AT, AU, AZ, BA, BB, BG, BH, BR, BW, BY, BZ, CA, CH, CN, CO, CR, CU, CZ, DE, DK, DM, DO, DZ, EC, EE, EG, ES, FI, GB, GD, GE, GH, GM, GT, HN, HR, HU, ID, IL, IN, IS, JP, KE, KG, KM, KN, KP, KR, KZ, LA, LC, LK, LR, LS, LT, LU, LY, MA, MD, ME, MG, MK, MN, MW, MX, MY, MZ, NA, NG, NI, NO, NZ, OM, PG, PH, PL, PT, RO, RS, RU, SC, SD, SE, SG, SK, SL, SM, ST, SV, SY, TJ, TM, TN, TR, TT, TZ, UA, UG, US, UZ, VC, VN, ZA, ZM, ZW.

(84) Designated States *(unless otherwise indicated, for every kind of regional protection available)*: ARIPO (BW, GH, GM, KE, LS, MW, MZ, NA, SD, SL, SZ, TZ, UG, ZM, ZW), Eurasian (AM, AZ, BY, KG, KZ, MD, RU, TJ, TM), European (AT, BE, BG, CH, CY, CZ, DE, DK, EE, ES, FI, FR, GB, GR, HR, HU, IE, IS, IT, LT, LU, LV, MC, MK, MT, NL, NO, PL, PT, RO, SE, SI, SK, TR), OAPI (BF, BJ, CF, CG, CI, CM, GA, GN, GQ, GW, ML, MR, NE, SN, TD, TG).

Published:

— *without international search report and to be republished upon receipt of that report (Rule 48.2(g))*

WO 2010/033267 A2

(54) Title: STRUCTURES, METHODS OF MAKING STRUCTURES, MULTI-WELL ARRAY SURFACE ENHANCED RAMAN SPECTROSCOPY (SERS) CHIPS, METHODS OF MAKING, AND METHODS OF USE

(57) Abstract: Embodiments of the present disclosure relate to structures having one or more wells that include nanorods and methods of making the structures.

STRUCTURES, METHODS OF MAKING STRUCTURES, MULTI-WELL ARRAY SURFACE ENHANCED RAMAN SPECTROSCOPY (SERS) CHIPS, METHODS OF MAKING, AND METHODS OF USE

CROSS-REFERENCE TO RELATED APPLICATION

This application claims priority to co-pending U.S. provisional application entitled "A Multi-Well Array Biochip for Multiplexing Surface Enhanced Raman Spectroscopy Analysis," having Serial No. 61/050,645, filed May 6, 2008, which is entirely incorporated herein by reference.

STATEMENT REGARDING FEDERALLY SPONSORED RESEARCH OR DEVELOPMENT

Aspects of this disclosure may have been made with government support under CMMI-072670 awarded by the National Science Foundation and W911NF-07-2-0065 awarded by the U.S. Army Research Laboratory. The government may have certain rights in the invention(s).

BACKGROUND

Biochemical and genetic diagnostic tests often require large numbers of samples either to test a large number of variables or to screen large sample populations. The reagents used in these assays can be very expensive, and the sample itself may not be available in large quantities; therefore, smaller reaction volumes and parallel testing are essential.

Array techniques such as immunoassays and DNA microarray chips have proven to be extremely successful in biological and genetic assays and are thoroughly documented in the literature and text books (Ekins, R.P., 1989. J. Pharm. Biomed. Anal. 7, 155-168; Schena, M., Shalon, D., Heller, R., Chai, A., Brown, P.O., Davis, R.W., 1996. Proc. Nat. Acad. Sci.93, 10614-10619, which are herein incorporated by

reference for the corresponding discussion). These methods, although well established, do suffer from a few major setbacks. For example, both immunoassays and DNA microarrays require careful sample handling and substrate preparation to acquire useful results. Due to such processes, they are relatively time-consuming, often requiring at least several hours to incubate samples with the capture molecules (*i.e.*, antibodies or single stranded DNA) so that a sufficient number can bind for detection. Several substrate-washing steps are then needed to remove excess reagents and to minimize the background signal. In addition, as with most molecular-labeling assays, these methods require extrinsic reporter molecules that allow only for indirect detection of the molecule of interest. Therefore, the investigators must know before hand what they are looking for, at least approximately, in order to design the probes. Thus, a minimal step, time-efficient, and label-free technique with high specificity and sensitivity would be preferred for array studies.

Surface-enhanced Raman scattering (SERS) is an analytical method based on vibrational spectroscopy, which can give a characteristic spectrum of a specific molecule. The method uses nanoscopically rough metallic surfaces to greatly enhance Raman scattering cross-section by molecules adsorbed onto the metal surface. The characteristic Raman spectrum can act as a fingerprint to directly identify molecules or bio-agents in proximity to the substrate. This is a distinct advantage to the limited ability of the aforementioned methods. Without the need for incubating, a sample can be analyzed much more quickly by simply placing it on the substrate and scanning. Beyond its experimental ease, SERS also offers a high degree of sensitivity and specificity. Detection of single molecules is possible, and the specificity of the

technique with biological samples has allowed, not only for species level discrimination of bacteria and viruses, but also strain discrimination within species.

Currently, there are two different SERS array techniques: extrinsic and intrinsic (Tripp, R.A., Dluhy, R.A., Zhao, Y.-P., 2008. Nanotoday 3, 39-45, which is herein incorporated by reference for the corresponding discussion). Similar to the labeling method of immunoassays and DNA chips, extrinsic detection generally uses antibodies or single stranded DNA to tether molecules of interest onto a SERS-active surface with a SERS reporter molecule for detection. For example, Rohr, *et al.* showed that the Raman dye p-dimethylamionasobenzene (DAB) could be covalently attached to an antibody, and could then be detected on silver electrodes via a sandwich-configured immunoassay (Rohr, T.E., Cotton, T., Fan, N., Tarcha, P.J., 1989. Anal. Biochem. 182, 388-398, which is herein incorporated by reference for the corresponding discussion). Ni, *et al.* covalently coupled antibodies specific for various IgG molecules to SERS-active gold nanoparticle colloids on which Raman labels were adsorbed. This allowed for Raman detection of the labels that were indirectly immobilized onto a substrate surface treated with IgG (Ni, J., Lipert, R.J., Dawson, B., Porter, M.D., 1999. Anal. Chem. 71, 4903-4908, which is herein incorporated by reference for the corresponding discussion). Jun, et al. designed a SERS reporter micro-complex using polymer microspheres embedded with silver nanoparticles on which SERS reporter molecules such as 4-methylbenzenethiol, 2-naphthalenethiol, and benzenethiol were adsorbed. The microbead/nanoparticle/reporter complex was then stabilized within a silica shell followed by coating with a bioactive molecule, such as biotin or antibody, that was shown to bind the respective bioantigens to the surface of the silica coated SERS bead

(Jun, B.-H., Kim, J.-H., Park, H., Kim, J.-S., Yu, K.-N., Lee, S.-M., Choi, H., Kwak, S.-Y., Kim Y.-K., Jeong, D.H., Cho, M.-Haing, Lee, Y.-S., 2007. J. Comb. Chem. 9, 237-244, which are herein incorporated by reference for the corresponding discussion). Although proven to be relatively successful, this extrinsic method relies on indirect detection, similar to the immunoassay and DNA microarrays discussed above; besides the advantages of a narrow spectral bandwidth and possible high sensitivity, the extrinsic method suffers from the same general disadvantages of the current array techniques.

There have been few reports to elicit methods for array-based SERS detection through intrinsic SERS substrates. Shin, *et al.* demonstrated that colloidal silver nanoparticles could be inked onto a silicon polymer stamp and printed onto a gold substrate coated with an organic self-assembled monolayer to yield an array of 50 μm × 50 μm square-shaped patterns. They then used the Raman label rhodamine G6 to demonstrate the SERS-enhancement generated in the micron patterned squares (Shin, H.S., Yang, H.J., Jung, Y.M., and Kim, S.B., 2002. Vib. Spectrosc. 29, 79-82, which is herein incorporated by reference for the corresponding discussion). However, when using nanoparticles on solid substrates, the SERS enhancement will depend on the monodispersion and aggregation of the nanoparticles. Furthermore, the patterning method does not provide an enclosure to contain a liquid sample from spreading across the substrate, leading to potential cross-contamination of samples. Bell, *et al.* developed a method of mixing silver colloidal nanoparticles with a liquid polymer, preferentially a polymer that has a small Raman cross-section, which was then deposited into the wells of a standard 96 well microtiter plate where the polymer/nanoparticle mixture was allowed to dry. Upon rehydration of the polymer with

an aqueous sample, the polymer swelled providing the analyte molecules access to the embedded nanoparticles for enhancement (Bell, S.E.J., Spence, S.J., 2001. Analyst 126, 1-3, which is herein incorporated by reference for the corresponding discussion). This study admittedly did have some limitations since only Raman-resonant molecules were analyzed, which suffered from poor signal reproducibility. Furthermore, this method may not be suitable for low-level detection since the polymer, although having a relatively small Raman cross-section, may still interfere with low signal detection of an analyte. Strop, et al. drop coated polymer nanobeads into the wells of a 96-well microtiter plate, allowing monolayers of the beads to form. Silver was then vapor deposited into the wells allowing silver thin films to form over the beads, creating a SERS active substrate. The study shows that the substrates show good reproducibility from well to well, but only relatively high concentrations of analyte were used (Stropp, J., Trachta, G., Brehm, G., and Schneider, S., "A new version of AgFON substrates for high-throughput analytical SERS applications," J. Raman Spectrosc. 34, 26-32 (2003).

The key to making SERS a practical array technique is the fabrication of uniform, higher enhancement, and larger area SERS substrates. Throughout the last thirty years, many different fabrication techniques have been explored in order to make high enhancement SERS substrates, including electrochemical oxidation reduction cycles (ORC), chemical etching, metal island films, electron beam lithography, and nanosphere lithography, to name a few. However, none of these techniques have been shown to produce large enough area, with high signal enhancement and uniformity that SERS substrates would be required for array techniques. They produce either relatively low enhancement and poor reproducibility but large surface area SERS substrates, such as

ORC, chemical etching, and metal island films; or large enhancement but small area sample, such as electron beam lithography and nanosphere lithography.

SUMMARY

Embodiments of the present disclosure relate to structures having one or more wells that include nanorods and methods of making the structures.

Briefly described, embodiments of the present disclosure include a structure comprising a substrate comprising at least one well, where the well has a bottom surface and a side surface, and where a plurality of nanorod structures are disposed on the bottom surface.

In an embodiment, a method of making a structure includes forming a well on a substrate, where the substrate includes a plurality of nanorods, where the well has a bottom surface and a side surface, and where a plurality of nanorod structures are disposed on the bottom surface.

BRIEF DESCRIPTION OF THE DRAWINGS

Many aspects of this disclosure can be better understood with reference to the following drawings. The components in the drawings are not necessarily to scale, emphasis instead being placed upon clearly illustrating the principles of the present disclosure. Moreover, in the drawings, like reference numerals designate corresponding parts throughout the several views.

FIG. 1A is a cross-sectional view of a structure including a well having nanorods disposed in the well.

FIG. 1B illustrates a cross-sectional view of another structure including a well having nanorods disposed in the well.

FIGS. 2A-2C illustrate a cross-sectional view of a method of making the structure shown in FIG.1A.

FIG. 3A illustrates the assembly of the well-patterning plate (1) mold with the SERS substrate (2) with the SERS active surface of the substrate facing the well-patterning plate. The PDMS is poured into the opening (3) between the substrate and well-patterning plate. The base and top plates of the mold assembly have been left out for clarity.

FIG. 3B illustrates a patterned substrate after removing from mold assembly with well labeling scheme. The wells within the dashed box are those analyzed for the leakage test.

FIG. 4 is a graph that illustrates Raman spectra from nine wells centered around well B8. The dashed spectrum corresponds to well B8 where BPE was added. The other eight spectra were taken from the other wells directly neighboring B8. The black arrow is pointing at the 1200 cm^{-1} BPE peak from well B8.

FIGS. 5A-5F illustrate I_{1200} mapping of each well of the 4 × 10 patterned substrate for the bare substrate, methanol only, 10^{-8} M, 10^{-7} M, 10^{-6} M, 10^{-5} M BPE, respectively. Well D10 is observably less intense than the other wells after the addition of BPE.

FIG. 5G illustrates a plot of the mean I_{1200} of the entire patterned substrate at each BPE concentration. The logarithmic grey scale corresponds to the average I_{1200} of each well with black corresponding to less intensity and white corresponding to higher intensity.

FIG. 5H illustrates a high resolution mapping of well B5 after the final 10^{-5}M BPE solution was added. It can be seen that the I_{1200} peak intensity is not completely uniform across the bottom surface of the well. Note that the grey scale for FIG. 5H is not logarithmic.

FIG. 6A is a graph that illustrates a log-log plot of thirty-nine wells at each concentration of BPE with linear fits for each well. The dark black line is a linear fit of the average peak intensities at each concentration with a slope of 0.57.

FIG. 6B is a graph that illustrates the apparent sensitivity of SERS enhancement relative to mole number of BPE under laser spot. The patterned substrate described in this disclosure is compared to the apparent sensitivity of the unpatterned OAD silver nanorod substrates from references (Chu, H., Liu, Y., Huang, Y., Zhao, Y.-P., 2007. Optics Exp. 15, 12230-12239, which is herein incorporated by reference for the corresponding discussion) and (Driskell, J.D., Shanmukh, S., Liu, Y., Chaney, S.B., Tang S.-J., Zhao Y.-P., Dluhy, R.A., 2008. J. Phys. Chem. C 112, 895-901, which is herein incorporated by reference for the corresponding discussion) to show that the apparent sensitivity is in the same general range. The dotted and dashed line correspond to the linear fits of data from Chu, *et al.* and Driskell, *et al*, respectively.

FIGS. 7A-7B illustrate representative AIV Raman spectra from (FIG. 7A) the patterned substrate and (FIG. 7B) the unpatterned 1×1 cm^2 substrate.

FIG. 7C is a graph that illustrates PC1 vs PC2 scatter plot for AF and AIV treated patterned and unpatterned substrates for PCA analysis.

FIG. 7D is a graph that illustrates Q-residual plots for the same samples from FIG. 7C.

FIG. 8 illustrates a dendogram of the allantonic control (AF) and influenza (Flu) samples on both patterned and unpatterned substrates.

FIG. 9A illustrates a diagram of the patterned substrate fabrication process. 1) Vapor deposition at 0° is used to deposit a 20 nm titanium thin film followed by 2) a 500 nm silver thin film onto a clean glass microscope slide. 3) The substrate is rotated 86° relative to the incident vapor and silver is further deposited allowing nanorod nucleations to form. 4) Continuous deposition at 86° allows the nucleations to form nanorods. 5) The substrate is placed in contact with the well-patterning mold and 6) PDMS is poured into the mold assembly. 7) After applying heat and sufficient time to cure, the PDMS forms solid yet flexible cast, allowing the well patterning-plate and substrate to be separated.

FIG. 9B illustrates the pattern molding process. The nanorod surface of substrate (1) is placed into contact with the well patterning plate (2). They are then pressed together between the top and bottom plates (3 and 4). PDMS is poured into the mold opening (5). After curing, the mold is disassembled and a forty well patterned substrate is ready to be used (6).

FIGS. 10A-10B illustrate I_{1200} (scaled 5×) plots of all forty wells of a 100°C cured substrate and a 50°C cured substrate prepared in the same deposition batch. The solid line is the mean I_{1200} and the dotted lines are one standard deviation above and below the mean.

FIGS. 11A-11B illustrate a comparison of cylindrical and conical wells. The solid line is the mean I_{1200} and the dotted lines are the standard deviation above and below the mean. The conical well intensities have been scaled 2.5×.

DETAILED DESCRIPTION

Before the present disclosure is described in greater detail, it is to be understood that this disclosure is not limited to particular embodiments described, as such may, of course, vary. It is also to be understood that the terminology used herein is for the purpose of describing particular embodiments only, and is not intended to be limiting, since the scope of the present disclosure will be limited only by the appended claims.

Where a range of values is provided, it is understood that each intervening value, to the tenth of the unit of the lower limit (unless the context clearly dictates otherwise), between the upper and lower limit of that range, and any other stated or intervening value in that stated range, is encompassed within the disclosure. The upper and lower limits of these smaller ranges may independently be included in the smaller ranges and are also encompassed within the disclosure, subject to any specifically excluded limit in the stated range. Where the stated range includes one or both of the limits, ranges excluding either or both of those included limits are also included in the disclosure.

Unless defined otherwise, all technical and scientific terms used herein have the same meaning as commonly understood by one of ordinary skill in the art to which this disclosure belongs. Although any methods and materials similar or equivalent to those described herein can also be used in the practice or testing of the present disclosure, the preferred methods and materials are now described.

All publications and patents cited in this specification are herein incorporated by reference as if each individual publication or patent were specifically and individually indicated to be incorporated by reference and are incorporated herein by reference to disclose and describe the methods and/or materials in connection with which the

publications are cited. The citation of any publication is for its disclosure prior to the filing date and should not be construed as an admission that the present disclosure is not entitled to antedate such publication by virtue of prior disclosure. Further, the dates of publication provided could be different from the actual publication dates that may need to be independently confirmed.

As will be apparent to those of skill in the art upon reading this disclosure, each of the individual embodiments described and illustrated herein has discrete components and features which may be readily separated from or combined with the features of any of the other several embodiments without departing from the scope or spirit of the present disclosure. Any recited method can be carried out in the order of events recited or in any other order that is logically possible.

The following examples are put forth so as to provide those of ordinary skill in the art with a complete disclosure and description of how to perform the methods and use the compositions and compounds disclosed and claimed herein. Efforts have been made to ensure accuracy with respect to numbers (*e.g.*, amounts, temperature, *etc.*), but some errors and deviations should be accounted for. Unless indicated otherwise, parts are parts by weight, temperature is in °C, and pressure is at or near atmospheric. Standard temperature and pressure are defined as 20 °C and 1 atmosphere.

Before the embodiments of the present disclosure are described in detail, it is to be understood that, unless otherwise indicated, the present disclosure is not limited to particular materials, reagents, reaction materials, manufacturing processes, or the like, as such can vary. It is also to be understood that the terminology used herein is for purposes of describing particular embodiments only, and is not intended to be limiting.

It is also possible in the present disclosure that steps can be executed in different sequence where this is logically possible.

It must be noted that, as used in the specification and the appended claims, the singular forms "a," "an," and "the" include plural referents unless the context clearly dictates otherwise. Thus, for example, reference to "a support" includes a plurality of supports. In this specification and in the claims that follow, reference will be made to a number of terms that shall be defined to have the following meanings unless a contrary intention is apparent.

Discussion

In accordance with the purpose(s) of the present disclosure, as embodied and broadly described herein, embodiments of the present disclosure, in one aspect, relate to structures having one or more wells that include nanorods and methods of making the structures. In an embodiment, the structure is a surface enhanced Raman spectroscopy (SERS) active substrate, where the nanorods can be fabricated by oblique angle deposition (OAD), for example. In an embodiment, the wells can be patterned by a material (*e.g.*, a polymer material) through different patterning techniques including, but not limited to a molding technique, a lithography method, a printing method, and a peeling method to provide a uniform array for high throughput biosensing and/or multiplexing.

In an embodiment, the substrate includes at least one well. In an embodiment, the substrate can include an array of wells. The well can have a bottom surface and a side surface or side wall. In an embodiment, the bottom surface and the side surface or

wall define the well, which is open on the top. In addition, a plurality of nanorod structures is disposed on the bottom surface of the well.

In an embodiment, the bottom surface can be the same material as the substrate. In another embodiment, the bottom surface is a material different than the substrate. In another embodiment, the bottom surface and the side surface are made of the same material or of different materials. In an embodiment, the substrate, the bottom surface, and the side surface are made of the same material or different materials.

In addition, embodiments of the present disclosure include a nanorod substrate multi-well array chip (*e.g.*, a structure including multiple wells) comprising a nanorod substrate, where wells are cast in a material (*e.g.*, a polymer) on the surface of the substrate. In an embodiment, the substrate is a surface-enhanced Raman spectroscopy (SERS) substrate. In another embodiment, the chip is used for the detection of at least one biomolecule in a sample. In another embodiment, the chip is a SERS multiplexing platform.

In an embodiment of the present disclosure, the wells are completely isolated from each other (*e.g.*, does not include channels connecting the wells or the channels can be closed) so that the samples are completely contained in a specific well (*e.g.*, confined in a lateral direction), which should reduce or eliminate cross-contamination between or among the wells. In an embodiment, each well acts as an isolated, independent SERS substrate capable of biomolecule detection. Biomolecules for detection include DNA, RNA, carbohydrates, proteins, coenzymes, cofactors, and the like. In an embodiment, one or more channels or other conduits can be used to connect

one or more of the wells to a fluid system to add or remove one or more fluids or reactants to the well.

In an embodiments of the present disclosure, a nanorod substrate multi-well array chip can have a detection limit of at least about 10^{-18} moles of 1,2-Di(4-pyridyl)ethylene ≥98% (BPE).

Embodiments of the present disclosure include nanorods selected from one of the following materials: a metal, a metal oxide, a metal nitride, a metal oxynitride, a polymer, a multicomponent material, and combinations thereof. In an embodiment, the material is selected from one of the following: silver, nickel, aluminum, silicon, gold, platinum, palladium, titanium, cobalt, copper, zinc, oxides of each, nitrides of each, oxynitrides of each, and combinations thereof. In an embodiment, the nanorods are made of silver.

In an embodiment, the nanorods can be formed using a modified oblique angle deposition (OAD) technique/system (additional details are described in U.S. Patent Application 2007/0166539, which is incorporated herein by reference). For example, the OAD system can include a two-axis substrate motion system in a physical vapor deposition (PVD) device (*e.g.*, thermal evaporation, e-beam evaporation, sputtering growth, pulsed laser deposition, and the like) that operates at temperatures lower than the melting point of the material used to form the nanorods. In an embodiment, the substrate motion system provides two rotation movements: one is the polar rotation, which changes angle between the substrate surface normal and the vapor source direction, and one is the azimuthal rotation, where the sample rotates about its center axis of rotation (*e.g.*, normal principle axis).

Embodiments of the OAD system can include a physical vapor deposition (PVD) device, such as thermal evaporation, e-beam evaporation, molecular beam epitaxy (MBE), sputtering growth, pulsed laser deposition, combinations thereof, and the like, to form the nanorods.

In an embodiment, the nanorods are in an array, and the array of nanorods can be defined as having a distance of about 10 to 30 nm, about 10 to 60 nm, about 10 to 100 nm, about 10 to 150 nm, or about 10 to 200 nm, between each of the nanostructures. Alternatively, the array of nanorods can be defined as having an average density of about 11 to 2500/μm^2.

The length is the largest dimension of the nanorod and is the dimension extending from the substrate. The nanorod can have a length of about 10 nm to 5000 nm, about 10 nm to 4000 nm, about 10 nm to 3000 nm, about 10 nm to 2000 nm, about 10 nm to 1000 nm, about 10 nm to 500 nm, about 10 nm to 250 nm, about 10 nm to 100 nm, or about 10 nm to 50 nm. The length depends, at least in part, upon the deposition time, deposition rate, and the total amount of evaporating materials. The diameter is the dimension perpendicular to the length. The diameter of the nanorod is about 10 to 30 nm, about 10 to 60 nm, about 10 to 100 nm, or about 10 to 150 nm. One or more of the dimensions of the nanorod could be controlled by the deposition conditions and the materials.

FIG. 1A is a cross-sectional view of a structure 10a including a well having nanorods 14 disposed in the well. In an embodiment, the well is defined on the bottom and sides by a substrate 12 (the bottom surface) and side walls 16 or side surfaces. In

an embodiment, a portion 18 of the well may not include nanorods. However, in another embodiment, the well does not include a portion such as that shown in FIG. 1A.

It should also be noted that FIG. 1A shows the angle, β, formed between the nanorod and the substrate. In an embodiment, the angle can be about 40° to 50 °, about 30 ° to 60 °, or about 30 ° to 75 °. The nanorods of each of the embodiments described herein can include an angle, β. The angle will help to promote the SERS "hot spot" sites on the surface, and increase the enhancement of SERS signals of the molecules located in-between the nanorods.

FIG. 1B is a cross-sectional view of another structure 10b including a well having nanorods disposed in the well. The structure 10b is similar to the structure 10a in FIG. 1A. The structure 10b includes a different design for the side wall or side surfaces. In other embodiments, the side wall or side surfaces can have other configurations or designs consistent with the use of embodiments of the present disclosure. It should also be noted that structure 10b does not include a portion 18 such as that shown in FIG. 1A.

In an embodiment, the side walls or side surfaces can be made of a material such as polymer. Embodiments of the present disclosure include polymers selected from the group consisting of: polydimethylsiloxane (PDMS), fluorinated PDMS, poly(methyl methacrylate) (PMMA), polycyclic olefin polyethylene copolymers, polycarbonate, polyalkanes, polyacrylate polybutanol co-polymers, polystyrenes, polyionomers, such as Surlyn® and Bynel®, polybutyl terephthalate (PBT), polyamides, such as nylons of different grades (*e.g.*, nylon 6-6, nylon, 6 nylon 6-12, etc.),

polyoxymethylene (POM), other acetyl resins polyurethane, and the like, combinations thereof, and similar polymers.

In an embodiment, the polymer can be PDMS. PDMS can be used because PDMS can be cured relatively quickly at low temperatures. After curing, the polymer is very stable and does not react or dissolve readily when in contact with organic solvents. Furthermore, PDMS retains the precise shape of the mold after curing and shows a sufficient ability to adhere to the nanorod surface of the substrate.

The number, arrangement, and volume of the wells can be changed, as well as the material to make the wells (*e.g.*, the standard 96-well or 48-well structure for biological analysis can be realized). This provides a direct, efficient way to screen large numbers of samples. In addition, embodiments of the present disclosure can be incorporated into other newly emerging technologies (*e.g.*, microfluidic systems), allowing for real-time and dynamic analysis of samples.

Embodiments of the present disclosure include wells that can be a shape selected from the group consisting of: cylindrical, conical, polygonal, and the like. The shape or dimensions of the well can be designed based on the configuration of the structure, uses of the structure, method of making the structure, materials used to make the structure and/or nanorods, and the like. Thus, embodiments of the present disclosure can include additional well shapes.

In an embodiment, each well has a bottom diameter of about 2 to 6 mm or about 4 mm, and a height of about 0.5 to 2 mm or about 1 mm. In an embodiment, the top of the conical well has diameter of about 2 to 6 mm or about 4 mm much like a cylindrical well, however, the bottom diameter (the edge in contact with the substrate) is about 1 to

3 or about 2 mm. In an embodiment, the height of the well can be about 0.25 to 2 mm or about 0.5 to 1 mm. In an embodiment, the height of the well can be 2 or more mm depending upon the design and/or use of the well. The dimensions of a particular embodiment can be tailored based on the configuration of the structure, uses of the structure, method of making the structure, materials used to make the structure and/or nanorods, and the like.

Embodiments of the present disclosure can include wells that can each contain up to about 14 µl volume of sample. In an embodiment, the wells can each contain up to about 12.6 µl volume of sample. In an embodiment, the wells can each contain about 1 to 12.6 µl volume of sample for the cylindrical wells. In an embodiment, the wells can each contain about 1 to 7.3 µl volume of sample for the conical wells. In an embodiment, the volume of the well can be tailored based on the configuration of the structure, uses of the structure, method of making the structure, materials used to make the structure and/or nanorods, and the like.

Embodiments of the present disclosure include about 2 to 100 wells cast in a polymer on the surface of the substrate.

Embodiments of the present disclosure can include uniform well to well Raman signal enhancement. In an embodiment, there may be less spectral variation using the patterned well disclosed herein. Although not intending to be bound by theory, the decrease in spectral variation in the multi-well patterned substrate may facilitate (or in combination with the sample type) reproducible spotting and drying of the sample in a well-defined area on the substrate.

Embodiments of the present disclosure can decrease the amount of actual SERS substrate required for sample analysis, thus, decreasing cost; allow high sensitivity and specificity for chemical and biochemical detection; aid in establishing a more uniform substrate for better reproducibility for SERS analysis; and/or allow for more automated and efficient sample analysis and data acquisition.

In an embodiment, the structure can be formed by forming a well on a substrate. In an embodiment, a well can be formed using mold casting methods such as those described in the Examples. In another embodiment, the well can be formed using other methods such as lithography, spin coating, adhering (via PDMS or some other polymer) pre-formed well arrays to the nanorod substrate, and the like. The well has a bottom surface and a side surface. As described above, the substrate includes a plurality of nanorods. A plurality of nanorod structures is disposed on the bottom surface.

In an embodiment, the substrate is provided, and a plurality of nanorods on the substrate can be disposed on the substrate prior to forming the well (*e.g.*, side surfaces or side walls) around the nanorods. In an embodiment, the material to form the well is disposed on a portion of the substrate (which may include nanorods), but is not disposed on a portion of the nanorods. In other words, the material to form the side surfaces or side walls is disposed around a plurality of nanorods. The material and the bottom surface define the well since the top of the well is open. It should be noted that if channels to the wells are included, the surface of opening when the opening is closed, is part of the bottom surface and/or the side walls or side surfaces. In an embodiment, the material can be cured or otherwise hardened so that the structure can be used in a SERS system.

FIGS. 2A through 2C illustrate a cross-sectional view of a method of making the structure shown in FIG.1A. FIG. 2A illustrates a substrate 12. FIG. 2B illustrates a layer of nanorods 14 formed on the substrate 12. In an embodiment, the nanorods 14 can be formed using OAD. FIG. 2C illustrates the formation of the side walls or side surfaces 16. In addition, a portion 18 of the substrate 12 surface does not include the side surface or side wall or the nanorods. In an embodiment, the side wall or side surfaces 16 can be formed using a mold casting system, which is described in the Examples. Additional details regarding the method for forming the structure are described in the Examples.

In another embodiment, the present disclosure includes a method of fabricating a microwell-arrayed SERS chip on a standard glass microscope slide using OAD to produce a SERS-active surface, followed by use of a well-array patterning mold in which liquid PDMS is added and cured by low temperature heating. In an embodiment, a mold allows for casting of the microwell pattern on the nanorod surface. Each positive well relief on the mold has a negative relief imprinted in its center, so as not to destroy the nanorod array of the substrate in the central portion of the bottom surface of the well during union of the substrate and mold. Consequently, there is a ring of inactivated substrate between the polymer wall of the well and the intact nanorod array on the bottom surface of each well.

As stated above, the SERS-active substrate (structure) is fabricated using OAD, and the microwell array is fabricated using a molding process. The molding process includes a well-patterning plate with protrusions and a base plate that holds the substrate in place (FIG. 9B). The patterning technique is flexible and allows for

patterning control and customization, as well as performance optimization of the substrate (*e.g.*, the protrusions can be varied in shape, size, and arrangement).

In another embodiment, the present disclosure includes a method of fabricating a nanorod substrate multi-well array chip comprising using OAD to produce a SERS-active substrate and using a well-array patterning mold, where a polymer is added and cured by low temperature heating. Low temperature heating includes room temperature to 100°C. It should be noted that higher temperatures may be needed for different polymers, for example PMMA may need higher temperature for curing. In an embodiment, the SERS-active substrate includes a silver (Ag) nanorod substrate.

As mentioned above, embodiments of the present disclosure include a polymer selected from the group consisting of: polydimethylsiloxane (PDMS), fluorinated PDMS, poly(methyl methacrylate) (PMMA), polycyclic olefin polyethylene copolymers, polycarbonate, polyalkanes, polyacrylate polybutanol co-polymers, polystyrenes, polyionomers, such as Surlyn® and Bynel®, polybutyl terephthalate (PBT), polyamides, such as nylons of different grades (*e.g.*, nylon 6-6, nylon, 6 nylon 6-12, etc.), polyoxymethylene (POM), other acetyl resins, and the like, combinations thereof, and similar polymers.

Embodiments of the present disclosure include patterning molds that can be customized for performance optimization. Additional details regarding the molds are described in the Examples.

In another embodiment, the present disclosure includes a method of fabricating a Ag nanorod SERS active substrate multi-well array chip comprising: depositing a 20 nm titanium thin film by vapor deposition at 0^{o} on a glass microscope slide; subsequently

depositing a 500 nm silver thin film; rotating the substrate 86° relative to an incident vapor; further depositing silver, allowing nanorods to form; placing the substrate in contact with a well-patterning mold; pouring PDMS into the mold assembly; applying heat and sufficient time to cure; and separating the well-patterning plate from the substrate once the PDMS forms a sturdy yet elastic cast. It should be noted that other metals and the like described above can be used in this method as well. In addition, other material (*e.g.*, polymers) described above can be used in this method as well. Other variables such as the dimensions, angles, and temperature can also be varied consistent with this disclosure.

EXAMPLES

Example 1

Introduction

Uniform, large surface area substrates for surface-enhanced Raman spectroscopy (SERS) were fabricated by oblique angle deposition. The SERS-active substrates are patterned by a polymer-molding technique to provide a uniform array for high throughput biosensing and multiplexing. Using a conventional SERS-active molecule, 1,2-Di(4-pyridyl)ethylene ≥98% (BPE), we show that this device provides a uniform Raman signal enhancement from well to well with a detection limit of at least 10^{-8} M of the BPE solution or 10^{-18} moles of BPE. The SERS intensity is also demonstrated to vary logarithmically with the log of BPE concentration and the apparent sensitivity of the patterned substrate is compared to previous reports from our group on non-patterned substrates. Avian influenza is analyzed to demonstrate the utility of SERS multi-well patterned substrates for biosensing. The spectra acquired from patterned substrates show better reproducibility and less variation compared to the

unpatterned substrates according to multivariate analysis. Our results highlight potential advantages of the patterned substrate.

Experimental

Materials

Standard 1" × 3" glass microscope Gold Seal® slides (Becton and Dickinson Company, catalog # 3010) were used as the starting substrate for the SERS chip. Titanium (99.995% pure) and silver (≥ 99.99% pure) were purchased from Kurt J. Lesker. PDMS (Sylgard® 184 Silicone Elastomer Kit) was obtained from Dow Corning. BPE was supplied by Fluka. Methanol ≥99.8% was obtained from Sigma-Aldrich.

SERS-active substrate fabrication

Glass slides were cleaned in heated piranha solution (4:1 v/v H_2SO_4:H_2O_2) for at least 10 minutes, and then thoroughly rinsed with DI water and blow dried with N_2. A custom-built electron beam evaporation chamber, used only in conjunction with titanium and silver, was employed to deposit titanium and silver onto the glass substrates similar to the method described previously (Driskell, J.D., Shanmukh, S., Liu, Y., Chaney, S.B., Tang S.-J., Zhao Y.-P., Dluhy, R.A., 2008. J. Phys. Chem. C 112, 895-901; Chaney, S.B., Shanmukh, S., Dluhy, R.A., Zhao, Y.-P., 2005. Appl. Phys. Lett. 87, 031908-1 – 031908-3, which are herein incorporated by reference for the corresponding discussion). All deposition rate and thickness measurements were determined by a quartz crystal microbalance (QCM) placed inside the chamber and facing the source material. The depositions were performed when the chamber reaches a base pressure of 10^{-6} torr. The surface of the substrate was positioned normal to the incident vapor.

A titanium adhesion layer was first deposited at a rate of 0.2 nm/s to a total QCM thickness reading of 20 nm. A silver thin film was deposited at a rate of 0.3 nm/s to a

total QCM thickness reading of 500 nm. The substrate was then rotated so that the surface normal was offset by 86° relative to the incident vapor. Silver was then deposited at a constant rate of 0.3 nm/s to a final QCM thickness reading of 2000 nm, to form a tilted Ag nanorod array. The substrates in the chamber were allowed to cool to room temperature in vacuum before they were removed from the chamber.

SERS array fabrication

The SERS array was fabricated using a molding process. The mold assembly was composed of a base plate that holds the substrate in place. The well-patterning plate (FIG. 3A) was machined from a single piece of aluminum with forty regularly spaced hollowed cylindrical protrusions arrayed in a 4 × 10 manner. Each protrusion has an outer diameter of 4 mm, a 0.5 mm thick radial wall, a hollowed inner diameter of 3 mm, and a height of 1 mm. Therefore, it is expected that each well formed with this mold will be able to contain a 12.6 μl volume of sample.

The protrusions prevent the PDMS from coating the SERS-active nanorods at the bottom of the well, which could interfere with the SERS response of the nanorod array. If the protrusion did not have a recessed central region, this would cause physical damage to the delicate nanorod array along the bottom of the well, which would also change the SERS signal response. Thus, there is a 0.5 mm thick ring of inactivated substrate along the edge of each patterned well.

The portion of the base plate to be in contact with the substrate/well-pattering plate was lined with a piece of wax paper to help the release of the substrate/PDMS/well-patterning plate from the bottom plate after curing. The PDMS base and the curing agent (10:1 wt/wt) were mixed together using a glass rod. Before

the liquid PDMS was added to the mold/substrate assembly, the assembly was first pre-heated in an oven at 100°C for 20 minutes. The PDMS was also preheated for 5 minutes and then poured into the opening of the substrate/mold assembly and allowed to cure at 100°C for approximately 20 minutes. After the substrate had cooled to room temperature, the well patterning plate was pulled off of the PDMS, leaving a uniform 4 × 10 well PDMS-patterned SERS-active microwell arrayed substrate as shown in FIG. 3B.

SERS chip characterization

The quality of the SERS array has been demonstrated through the following methods: (1) leakage test; (2) uniformity test; (3) sensitivity test; and (4) bioagent detection test.

Leakage test

One of the goals of the array SERS chip is to design microwells that can be isolated from each other so that the samples will be completely contained in a specific well without cross-contaminating the adjacent wells. In order to determine whether minute amounts of analyte were able to leak out of the well underneath the PDMS layer and through the silver nanorod layer, 5μl of a relatively concentrated BPE in methanol solution (10^{-4} M) was added to well B8 of a patterned SERS substrate (FIG. 3B). BPE was used because it has a large Raman cross section with its major spectral Raman peaks at 1008 cm^{-1}, 1200 cm^{-1}, 1338 cm^{-1}, 1604 cm^{-1} and 1640 cm^{-1}, respectively. BPE also adsorbs irreversibly onto Ag surfaces, and has been previously studied extensively for Ag nanorod SERS substrates (Yang, W., Hulteen, J., Schatz G.C., and Van Duyne, R.P., 1994. J. Chem. Phys 104, 4313-4323; Chaney, S.B., Shanmukh, S., Dluhy, R.A., Zhao, Y.-P., 2005. Appl. Phys. Lett. 87, 031908-1 – 031908-3; Chu, H., Liu, Y., Huang,

Y., Zhao, Y.-P., 2007. Optics Exp. 15, 12230-12239; Driskell, J.D., Shanmukh, S., Liu, Y., Chaney, S.B., Tang S.-J., Zhao Y.-P., Dluhy, R.A., 2008. J. Phys. Chem. C 112, 895-901, which are herein incorporated by reference for the corresponding discussion). Methanol is used as a solvent for BPE because it evaporates quickly and has a very good ability to spread on the silver nanorod array surface.

Well B8 with BPE solution was then covered with a small glass cover slip just large enough to fit over the well to inhibit evaporation of the methanol solution. Keeping the well filled with analyte solution for an extended time allows the seal formed between the PDMS and the silver nanorod film to be more rigorously evaluated. After 1.5 hours the methanol appeared to have evaporated and the glass coverslip was removed and any remaining methanol was allowed to dry. The SERS spectrum of well B8 along with the spectrum of the adjacent wells (FIG. 3B) were measured with an Enwave Fiber Raman probe system with an incident wavelength of 785 nm and an input power of 35-45 mW. Each scan had an integration time of 10 s and each output spectrum was set to be an average of two collected spectrums.

Uniformity and sensitivity test

All the SERS mapping measurements were carried out on a Renishaw inVia Raman microscope system equipped with an automated high precision actuation stage. For the SERS patterned substrate mapping, each well was measured in three separate spots. The second and third spots were + 0.5/ +0.5 mm (forward/up) and -0.5/-0.5 mm (backwards/down) relative to center (spot 1). Each spot was scanned with a 5× objective, 10% power, 785 nm excitation wavelength and 5 s acquisition time unless otherwise stated. A spectral range from 1130 to 1650 cm^{-1} was collected at each spot.

We used the 1200 cm^{-1} peak intensity, I_{1200}, to quantify the SERS response. The Renishaw's software was programmed to analyze the peaks using a mix of Gaussian and Lorenzian curves. The substrate analyzed by the Renishaw system was mapped within 72 hours of fabrication. For the well-to-well mapping, any spectral acquisitions that visually appeared to have a cosmic radiation (instrument noise) spike at 1200 cm^{-1} were removed from the analysis and only two points for that well were used for a single mapping, but only one spike at 1200 cm^{-1} was observed during the entire experiment.

The uniformity and sensitivity of the SERS array were characterized by measuring the SERS spectra while consecutively increasing the BPE concentrations. The first mapping demonstrates the response of the patterned substrate before the addition of any methanol or BPE. Then 5μl of methanol was added to each well of this same substrate and allowed to dry, and again the SERS response of the substrate was mapped. This was repeated using 5 μl of 10^{-8} M BPE added to each well of the same substrate, followed by the addition of 10^{-7}, 10^{-6}, and 10^{-5} M BPE. Sequentially increasing the concentration of the BPE solutions allowed the wells to be evaluated at multiple concentrations, but due to accumulation of the analyte it should be noted that after adding 1×10^{-7}, 1×10^{-6}, and 1×10^{-5} M BPE, the effective concentration in each well was 1.1×10^{-7}, 1.11×10^{-6}, and 1.111×10^{-5} M BPE, respectively.

In order to determine the uniformity across the SERS-active surface of the bottom of a well, a high resolution SERS mapping was performed on well B5. The well was scanned at over 6000 spots with a step size of 50 microns. The acquisition time was 2.5 s per spectral acquisition.

Virus detection

To test the virus detection capability of the SERS multiwell patterned substrate, avian influenza virus (AIV) was used. An AIV (H5N2 strain) isolate was propagated in embryonated chicken eggs. Allantoic fluid was harvested 48 hr post infection and the virus titer was measured to be 1.8 x 10^6 pfu/mL by plaque assay. Allantoic fluid (AF) collected from mock-infected (*i.e.*, PBS) embryonated chicken eggs served as a negative control sample.

Influenza-positive and negative allantoic fluid samples were diluted 100-fold prior to application to the SERS substrate. Allantoic fluid is a rather complex and concentrated background matrix, and when applied without dilution, multilayers formed on the nanorod substrate, quenching the SERS signal. To compare the results obtained from patterned SERS substrates to individual 1×1 cm^2 SERS substrates, 2.0 µL of each of the samples were applied to two different 1×1 cm^2 SERS substrates and three wells on a patterned substrate. Five spectra were recorded for each sample spotted on a substrate or spotted in a well.

SERS spectra were acquired using a Bruker Senterra Raman confocal microscope system. A 785 nm near-IR diode laser was used as the excitation source. The laser was focused into 5 µm diameter spot using a 20× objective, and the laser power at the sample surface was set at 24 mW. SERS spectra over the range of 430-1830 cm^{-1} were collected using the high resolution (3-5 cm^{-1}) grating (1200 lines/mm) and 10 s exposure.

Results and Discussion

Leakage test

A multi-well assay plate must be able to confine and isolate the contents of each well to prevent cross contamination of samples. For the leakage test, the SERS spectra of the well B8 soaked with BPE, and the eight wells adjacent without BPE are collected as shown in FIG. 4. BPE signatures were only observed in the well B8 where BPE was directly added and not in any of the eight adjacent wells; therefore, the wells are concluded to sufficiently confine the sample in the lateral direction on the SERS-active substrate surface. The leakage test has also been performed on well C3 and similar results are obtained.

Uniformity and sensitivity tests

The well-to-well uniformity and sensitivity are characterized by measuring the three-point mean SERS I_{1200} in each well. FIGS. 5A-5F show the average I_{1200} map for 4×10 well array for different concentrations of BPE, along with the background signal. Well D10 shows a relatively low I_{1200} at all BPE concentrations compared to the other wells, and we conclude that the enhancement in that well has been inhibited, and therefore, this well is considered an outlier. This does not appear to be an anomaly, since many of the SERS chips fabricated in our lab with this method appear to have relatively low enhancement in one or more of the corner wells. Without being bound by any particular theory, this may be prescribed as a fabrication optimization issue and is probably a result of the corner wells having more thermal contact with the heated mold during the curing process.

For the patterned substrate, before the addition of methanol or BPE, the mean background I_{1200} for the patterned substrate is 32 counts with a standard deviation of

±14 counts or 44%. With the addition of methanol, the mean background peak intensity increases to 56 counts with a standard deviation of ± 42 counts or 86%, with only one well reporting an I_{1200} signal over three standard deviations above the mean. The I_{1200} before the addition of BPE appears to be due to noise from the system and small contaminant peaks near 1200 cm^{-1}. Clearly, the I_{1200} (baseline corrected) is increasing after the addition of methanol but the exact reason for this is not completely understood. Without being bound by any particular theory, we believe this may be due to the dissolving of the ambient contamination into the methano,l and upon evaporation the contamination is redistributed at the base of the nanorods where Raman enhancement has been shown to be greater (unpublished data). The background signal is therefore defined to be the I_{1200} of the substrate after methanol but before BPE is added. After the addition of 10^{-8} M BPE, the SERS spectra of BPE is visible in all thirty-nine wells and the mean intensity is found to increase to 909 counts with a standard deviation of ± 412 counts or 45%, with 100% of the wells reporting a signal above three standard deviations of background excluding the outlier, well D10. The lower limit of detection for each well is therefore assumed to be at least 10^{-8} M BPE. The mean I_{1200} and standard deviation for the remaining 10^{-7}, 10^{-6}, and 10^{-5} M BPE solutions are 5495 ± 2203 (40%), 21149 ± 7653 (36%), and 49101 ± 11673 (24%), respectively, (FIG. 5G).

We also observe that the SERS signal within a single well varies. There are several possible explanations for such a variation of SERS signal across the bottom of the well. One possibility is that the nanorod array is not uniform across the entire substrate; the other possibility is that the BPE is being unevenly deposited across the nanorod surface at the bottom of the well during the spreading and drying process. To

investigate this, we performed a high resolution scan of one of the wells. FIG. 5H is a high (50 micron step) resolution I_{1200} mapping of the well B5 after all BPE concentrations were added (*i.e.*, 1.111×10^{-5} M). The area along the edge of the well appears to have a higher signal intensity. This area appears to coincide with the ring of solvent that forms along the edges of the well as the well dries, which has a tendency to dry first at the center; therefore, one may expect to find the BPE more concentrated along the edge where the well dries last. Thus, we conclude that the non-uniformly spreading or drying of BPE on the surface could contribute significantly to the SERS signal variations, and therefore the location within a well is a factor affecting signal intensity.

The SERS intensity at the $1200cm^{-1}$ band versus BPE concentration c for the 39 active wells (excluding well D10) are plotted in a log-log scale in FIG. 6A. There appears to be a linear relationship between log I_{1200} and log c, from which we define an apparent sensitivity α,

$$\alpha = \frac{\Delta \log I_{1200}}{\Delta \log c}.$$

The mean slope of the thirty-nine curves is 0.58, with a standard deviation of ± 0.07 or 12.1%, which shows a uniform response for all wells. In order to allow for comparison of this apparent sensitivity with other reports from our group, the number of moles of BPE within the laser spot area, which for the 5× objective of the Renishaw system is 1265 μm^2, was calculated assuming that the BPE solution was deposited uniformly across the bottom of the 4 mm diameter well (including the 0.5 mm SERS-inactive PDMS ring along the outer edge of the well). The average I_{1200} of thirty-nine wells

versus the mole number is plotted in FIG. 6B along with two sets of data from our previous studies on a 1 × 1 cm^2 unpatterned substrate (Chu, H., Liu, Y., Huang, Y., Zhao, Y.-P., 2007. Optics Exp. 15, 12230-12239; Driskell, J.D., Shanmukh, S., Liu, Y., Chaney, S.B., Tang S.-J., Zhao Y.-P., Dluhy, R.A., 2008. J. Phys. Chem. C 112, 895-901, which are herein incorporated by reference for the corresponding discussion). All of the data shown in FIG. 6B demonstrate a linear relationship between log I_{1200} and log N, where N is the mole number of BPE, and the apparent sensitivity α for unpatterned substrates is 0.38 and 0.37, respectively. The use of different instruments and experimental parameters for each of these studies make a direct comparison difficult, however, it does appear that the apparent sensitivity α for the patterned substrate falls into the same general range as that of the unpatterned substrates.

Viral SERS detection

The virus detection capability of the multiwell patterned chip has been evaluated by a strain (H5N2) of AIV and compared to that from the flat 1 × 1 cm^2 unpatterned substrate. It should be noted that the samples spread on the 1 × 1 cm^2 chips in an uncontrollable and irreproducible fashion, unlike the patterned substrates in which the sample is confined to a well-defined area. FIGS. 7A and 7B show the representative spectra of the AIV samples on both patterned and unpatterned substrates. Cursory examination of the SERS spectra reveals three important findings. First, AIV spectra collected on the patterned and unpatterned substrates are similar. Likewise, spectra of AF is also independent of the sensing substrate. Second, less spectral variation for the same sample is found for samples deposited in the wells as compared to the samples deposited on the 1 × 1 cm^2 unpatterned substrates. Third, similar SERS spectra for the

AIV and AF samples are observed (data not shown). This is not surprising since the AIV-positive sample largely consists of the same components as AF. However, closer investigation reveals several significant spectral features attributed to AIV in the spectra of the AIV samples but not the AF samples.

Multivariate methods of data analysis aid in the interpretation of these spectra, and confirmation of the observations alludes to above due to the complex nature of the SERS spectra and similarity of the spectra for positive and negative samples. Principal component analysis (PCA) has been applied to visualize the clustering of the data according to class (*e.g.*, AF-well, Flu-well, AF-unpatterned, Flu-unpatterned). A plot is generated to view the scores of PC1 versus PC2, as shown in FIG. 7C. Note that the spectra cluster according to the classes defined above, which confirms that SERS spectra allow for identification of biological samples. For the purpose of this work, however, it is the spread of the data points within each class that is of importance. Note that the spread of scores along PC1 is greater for the spectra collected from the chips compared to the patterned wells. The same trend is observed for the scores on PC2.

PCA reduces the dimensionality of the data, and while tightly clustered data in a PC scores plot suggests minimal signal variation, it does not implicitly confirm minimal variation among samples. The information not captured by the PCs could potentially vary significantly and would not be observed in a PC scores plot. Therefore, the spectral information not included in the PCA model must be evaluated. Q residual quantifies the information not described by the model. In other words, even if the data cluster tightly in the 2-D PC scores plots, large Q residual values suggest the data are not as similar as perceived. The Q residual for the AIV and AF spectra is shown in FIG.

7D. This plot reveals much larger Q residual values for the spectra collected from the unpatterned substrates compared to the patterned wells. This can be interpreted that more of the spectral information for the spectra collected on the unpatterned substrates is not described by the model and greater variance in the SERS signal is present than is observed in the 2-D scores plots above. This analysis definitively confirms that greater spectral variation is obtained from the chips than the patterned wells.

Hierarchical cluster analysis (HCA) has been applied to quantify the similarity among the spectra. The results are displayed in the dendogram (FIG. 8). This dendogram is generated using the Euclidean distance between furthest neighbors in real space, not PC space. Therefore, the total spectral variability is observed. The dendogram shows that the distance from the furthest neighbor for the spectra collected in the patterned wells is ~0.28, and for the spectra collected on unpatterned substrates is ~0.54-0.70, which demonstrates that the spectra from the multiwell substrate have less variation.

Each of these methods of spectral analysis results in the same conclusion; less spectral variation within a sample is obtained using a patterned well. We attribute this phenomenon to sampling and not differences in the nanorod structures. The multiwell patterned substrate facilitates reproducible spotting and drying of the sample in a well-defined area on the substrate. Variations in sample spreading and drying, as is observed for the 1×1 cm^2 unpatterned substrates, can lead to slight variations in the SERS spectra. Admittedly, however, the slight increase in spectral heterogeneity on the unpatterned substrates may be insignificant for many studies, as these substrates have been successfully employed for the classification of several viruses and differentiation of

viral strains (Shanmukh, S., Jones, L., Driskell, J.D., Zhao, Y.-P., Dluhy, R.A., Tripp, R.A., 2006. Nano Lett. 6, 2630-2636, which is herein incorporated by reference for the corresponding discussion).

Conclusion

Using OAD and low temperature polymer mold patterning method, a robust, uniform, patterned SERS multiwell chip has been fabricated and its ability to handle analysis of the representative analyte BPE has been evaluated. The results show that each active well has very similar SERS behavior using a Raman probe molecule. The virus detection capability for the multi-well chip is better than the unpatterned SERS substrate in terms of reproducibility and variations, which is of great advantage to develop the SERS chip as a multiplexing platform. All of these advantages can help the incorporation of Raman spectroscopy as a mainstream, highly sensitive analytical tool allowing for the commercialization and widespread use of SERS substrates, which currently do not exist due to the intrinsic difficulties of processing such devices. This multi-well SERS chip can decrease the amount of actual SERS substrate required for sample analysis, thus decreasing cost, allow high sensitivity and specificity for chemical and biochemical detection, aid in establishing a more uniform substrate for better reproducibility for SERS analysis, and allow for more automated and efficient sample analysis and data acquisition.

Example 2

Introduction

A second well-patterning plate was also designed in a similar manner, but the protrusions were conical shaped. The base of the protrusion was 3.25 mm, and the

walls were tapered at 45°, leaving a 1.5 mm diameter recessed region in the middle of the protrusion.

We have observed that the nanorod substrate loses SERS enhancement after being incubated at 100°C temperatures. In order to circumvent this problem, we mixed a cure-accelerator (5% by weight) with the PDMS before pouring into the mold that allows the polymer to cure at 50°C in roughly the same period of time as that of the standard PDMS at 100°C.

Patterned Substrate Optimization

In order to compare the low temperature (50°C) curing technique, two 1" × 3" substrates were fabricated in the same deposition batch. One substrate was patterned at 100°C and the other at 50°C. 5 µL of 10^{-5} BPE was added to each well and allowed to dry. Three points in each well were then mapped in a manner similar to that described in Example 1 but used a 1 second acquisition time.

We also investigated the effect of the shape of the mold on the SERS nanorod substrate. We compared the effect of the cylindrical and conical well structure. Again, two 1" × 3" substrates were fabricated in the same deposition batch, and both were molded with the 50° C technique, but one was patterned with a mold with cylindrical protrusions, and the other with conical protrusions. 5 µL of 10^{-5} BPE was added to each well and allowed to dry. Three points in each well were them mapped in a manner similar to that described Example 1. The conical wells demonstrated much higher enhancement, with the 1200 cm^{-1} peak actually saturating the detector at many points. Thus, to allow for more accurate peak fittings, the exposure for the conical well scans was decreased to 2 seconds so that the 1200 cm^{-1} peak did not saturate the detector.

The I_{1200} for the conical wells were therefore scaled by 2.5 so that they could be compared to the I_{1200} of the cylindrical wells.

After adding 10^{-5} M BPE to each well, the 50°C patterned substrate shows both a better mean I_{1200} (18513 counts) and a smaller well-to-well standard deviation (± 5686 counts or 30.7%) compared to that of the 100°C patterned substrate with 12171 ± 7130 (58.6%) counts (FIG. 10).

To test the difference of the I_{1200} in conical and cylindrical wells, a substrate of each type was fabricated using the 50°C process. After 5 μl of 10^{-5} M BPE was added and each well scanned at three points, the mean I_{1200} and standard deviation are compared (FIG. 11). The conical well substrate shows a mean I_{1200} (scaled 2.5 ×) of 102630 counts with a standard deviation of ± 28724 (28.0%), whereas the cylindrical well substrate has a mean I_{1200} of 34404 counts and a standard deviation of ± 2255l (65.5%).

We also observe that the SERS signal within a single well varies. This is likely due to the uneven drying of the sample solution within the well. As the methanol evaporates, the droplet shrinks and 'pools' in one spot, usually along the bottom edge of the well, thus increasing the amount of BPE deposited onto the silver nanorods in this area and forming a spot with higher intensity. The conical wells demonstrate a better ability to allow the MeOH droplet to stay more centered and uniformly distributed across the silver nanorod array on the bottom surface of the well as it dries. The uniformity of the wells is quantified by comparing the standard deviations of the three points scanned within each well to the mean I_{1200} for that well. For the forty wells of the cylindrical substrate, the mean percent standard deviation of the three points scanned within the

well to the mean I_{1200} of that well is 89.2%, whereas the conical substrate demonstrates a better mean percent standard deviation of only 26.1%.

One should note that the intensity and standard deviations for the patterned substrates from different batches may not correspond directly, such as when comparing the low temperature (50°C) cylindrical well substrate from FIG. 10 to that of FIG. 11. This is likely due to the intrinsic batch-to-batch variations of the OAD SERS substrates along with the variations that can occur from instrument calibration from day to day.

The above findings suggest that the temperature of the curing step and the shape of the wells can be adjusted to allow for higher signal intensity. Furthermore, adjusting these fabrication parameters appears to provide freedom to engineer an arrayed substrate to yield a more uniform distribution of an analyte across the SERS active surface within the wells.

It should be noted that ratios, concentrations, amounts, and other numerical data may be expressed herein in a range format. It is to be understood that such a range format is used for convenience and brevity, and thus, should be interpreted in a flexible manner to include not only the numerical values explicitly recited as the limits of the range, but also to include all the individual numerical values or sub-ranges encompassed within that range as if each numerical value and sub-range is explicitly recited. To illustrate, a concentration range of "about 0.1% to about 5%" should be interpreted to include not only the explicitly recited concentration of about 0.1 wt% to about 5 wt%, but also include individual concentrations (*e.g.*, 1%, 2%, 3%, and 4%) and the sub-ranges (*e.g.*, 0.5%, 1.1%, 2.2%, 3.3%, and 4.4%) within the indicated range. The term "about" can include ±1%, ±2%, ±3%, ±4%, ±5%, ±6%, ±7%, ±8%, ±9%, or

±10%, or more of the numerical value(s) being modified. In embodiments where "about" modifies 0 (zero), the term "about" can include ±1%, ±2%, ±3%, ±4%, ±5%, ±6%, ±7%, ±8%, ±9%, ±10%, or more of 0.00001 to 1. In addition, the phrase "about 'x' to 'y'" includes "about 'x' to about 'y'".

It should be emphasized that the above-described embodiments of the present disclosure are merely possible examples of implementations, and are merely set forth for a clear understanding of the principles of the disclosure. Many variations and modifications may be made to the above-described embodiments. All such modifications and variations are intended to be included herein within the scope of this disclosure and protected by the following claims.

CLAIMS

Therefore, at least the following is claimed:

1. A structure comprising:

a substrate comprising at least one well, wherein the well has a bottom surface and a side surface, and wherein a plurality of nanorod structures are disposed on the bottom surface.

2. The structure of claim 1, wherein the bottom surface is a different material than the side surface.

3. The structure of claims 1 or 2, wherein the side surface is made of a material selected from the group consisting of: polydimethylsiloxane (PDMS), fluorinated PDMS, poly(methyl methacrylate) (PMMA), polycyclic olefin polyethylene copolymers, polycarbonate, polyalkanes, polyacrylate polybutanol co-polymers, polystyrenes, polyionomers, polybutyl terephthalate (PBT), polyamides, polyoxymethylene (POM), other acetyl resins, and a combination thereof.

4. The structure of any one of claims 1 to 3, wherein the bottom surface is made of a silicon material.

5. The structure of any one of claims 1 to 4, wherein the material of the nanorod is selected from the group consisting of: a metal, a metal oxide, a metal nitride, a metal oxynitride, a polymer, a multicomponent material, and a combination thereof.

6. The structure of claim 5, wherein the material of the nanorod is selected from the group consisting of: silver, nickel, aluminum, silicon, gold, platinum, palladium, titanium, cobalt, copper, zinc, an oxide of each, a nitride of each, an oxynitride of each, and a combination thereof.

7. The structure of any one of claims 1 to 6, wherein each well includes up to about 14 µl volume of a sample.

8. The structure of any one of claims 1 to 7, wherein the structure is a surface-enhanced Raman spectroscopy (SERS) substrate.

9. The structure of any one of claims 1 to 8, wherein the wells are a shape selected from the group consisting of: a cylindrical shape, a conical shape, a polygonal shape, and a combination thereof.

10. The structure of any one of claims 1 to 9, wherein the wells confine a sample in the lateral direction of the substrate to prevent cross-contamination of each sample in each of the wells.

11. The structure of any one of claims 1 to 10, wherein the structure is a SERS multiplexing platform.

12. The structure of any one of claims 1 to 11, wherein the nanorod has a length of about 10 nm to 1000 nm.

13. The structure of any one of claims 1 to 12, wherein the nanorod has a diameter of about 10 to 200 nm.

14. The structure of any one of claims 1 to 13, wherein the nanorods are about 20 to 200 nm from one another.

15. The structure of any one of claims 1 to 14, wherein the substrate and the nanorod have an angle, β, between them from about 30 to 70 degrees.

16. A method of making a structure, comprising:

forming a well on a substrate, wherein the substrate includes a plurality of nanorods, wherein the well has a bottom surface and a side surface, and wherein a plurality of nanorod structures are disposed on the bottom surface.

17. The method of claims 16, further comprising:

providing a substrate; and

disposing a plurality of nanorods on the substrate.

18. The method of any one of claims 16 to 17, further comprising:

disposing a material onto a portion of the substrate, wherein the material is not disposed on a portion of the plurality of nanorod structures so that the material is disposed around a plurality of nanorod structures to form the well.

19. The method of any one of claims 16 to 18, wherein the bottom surface is a different material than the side surface material.

20. The method of any one of claims 16 to 19, wherein the side surface is made of a material selected from the group consisting of: polydimethylsiloxane (PDMS), fluorinated PDMS, poly(methyl methacrylate) (PMMA), polycyclic olefin polyethylene copolymers, polycarbonate, polyalkanes, polyacrylate polybutanol co-polymers, polystyrenes, polyionomers, polybutyl terephthalate (PBT), polyamides, polyoxymethylene (POM), other acetyl resins, and a combination thereof.

21. The method of any one of claims 16 to 20, wherein the bottom surface is made of a silicon material.

22. The method of any one of claims 16 to 21, wherein the material of the nanorod is selected from the group consisting of: a metal, a metal oxide, a metal nitride, a

metal oxynitride, a polymer, a multicomponent material, and a combination thereof.

23. The method of any one of claims 16 to 22, wherein the material of the nanorod is selected from the group consisting of: silver, nickel, aluminum, silicon, gold, platinum, palladium, titanium, cobalt, copper, zinc, an oxide of each, a nitride of each, an oxynitride of each, and a combination thereof.

24. The method of any one of claims 16 to 23, wherein each well includes up to about 14 µl volume of a sample.

25. The method of any one of claims 16 to 24, wherein the material is disposed on a portion the substrate using a mold.

26. The structure of any one of claims 16 to 25, wherein the nanorod has a length of about 10 nm to 1000 nm.

27. The structure of any one of claims 16 to 26, wherein the nanorod has a diameter of about 10 to 200 nm.

28. The structure of any one of claims 16 to 27, wherein the nanorods are about 20 to 200 nm from one another.

29. The structure of any one of claims 16 to 28, wherein the substrate and the nanorod have an angle, β, between them from about 30 to 70 degrees.

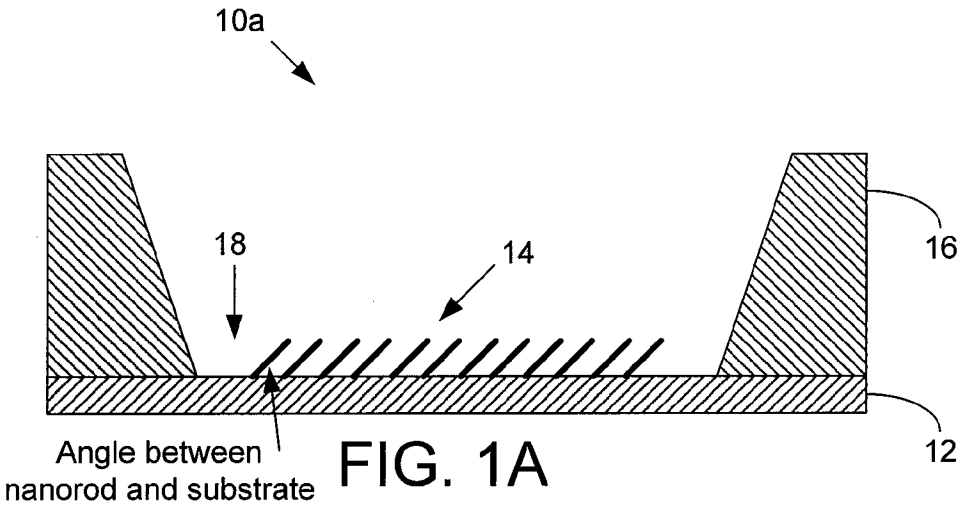
10a
18
14
16
12
Angle between
nanorod and substrate

FIG. 1A

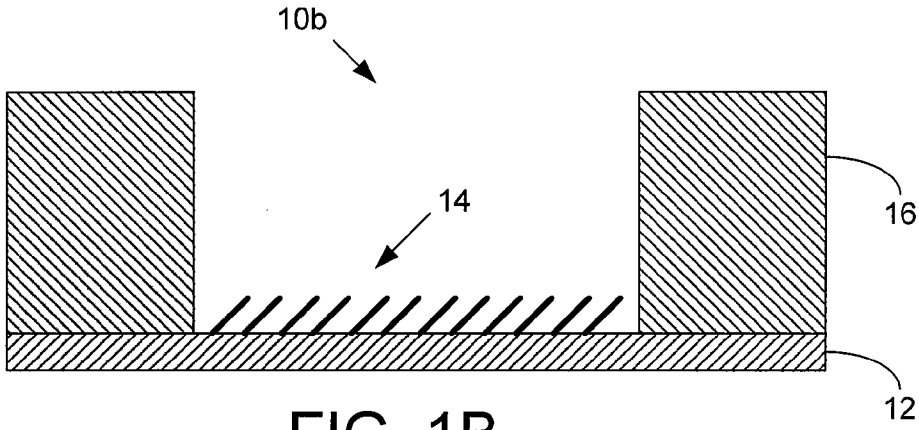
10b
14
16
12

FIG. 1B

FIG. 2A

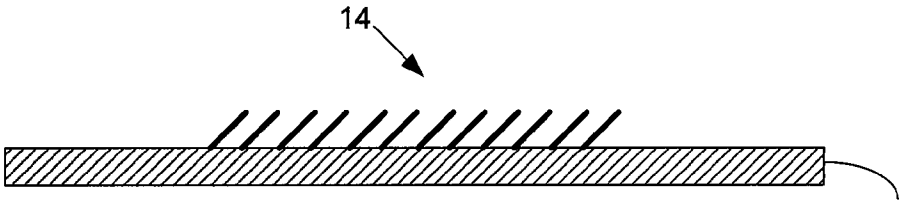

FIG. 2B

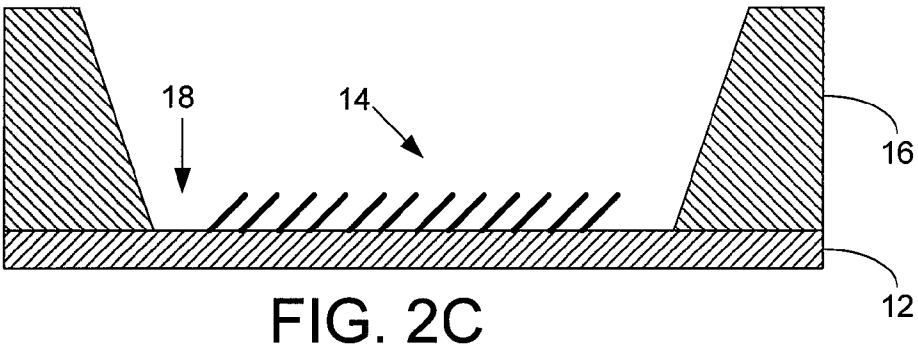

FIG. 2C

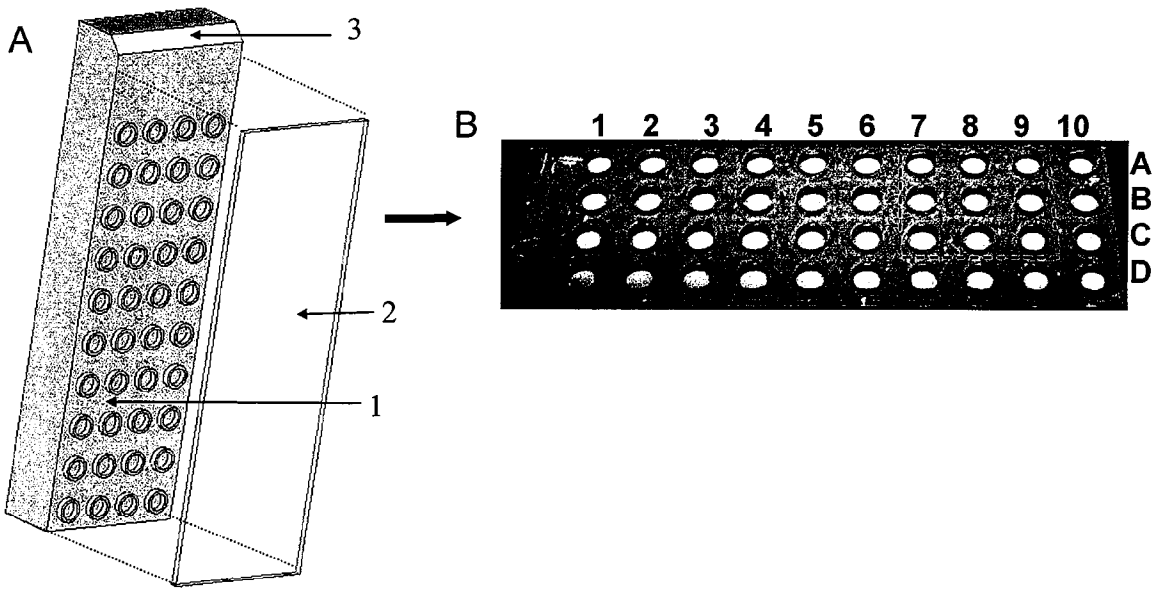

FIG. 3

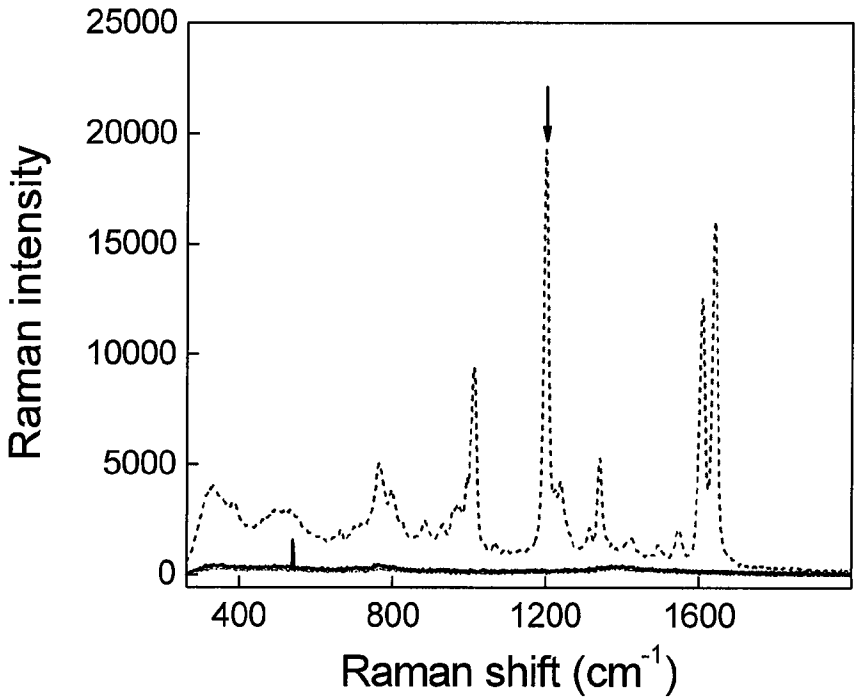
25000
20000
15000
10000
5000
0
Raman intensity
400
800
1200
1600
Raman shift (cm-1)

FIG. 4

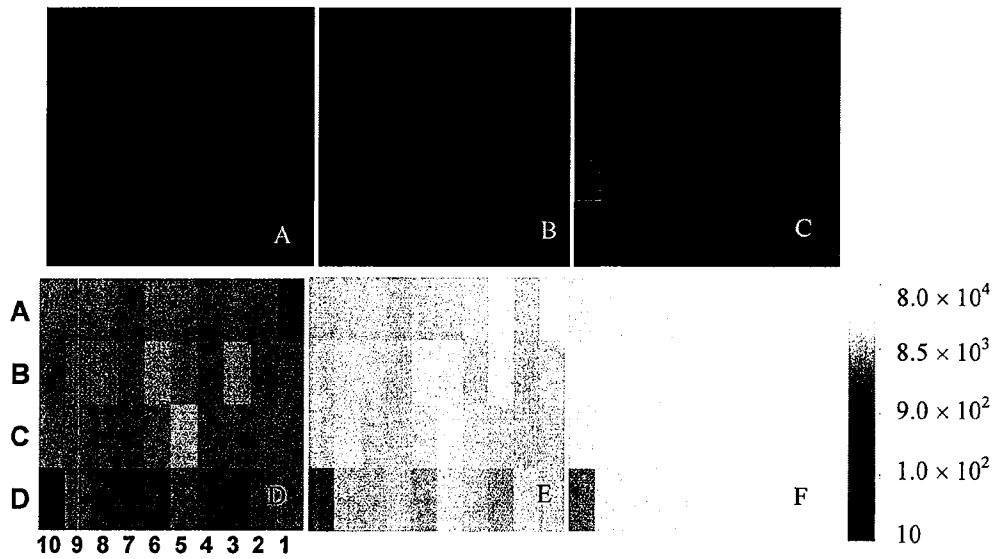

FIG. 5

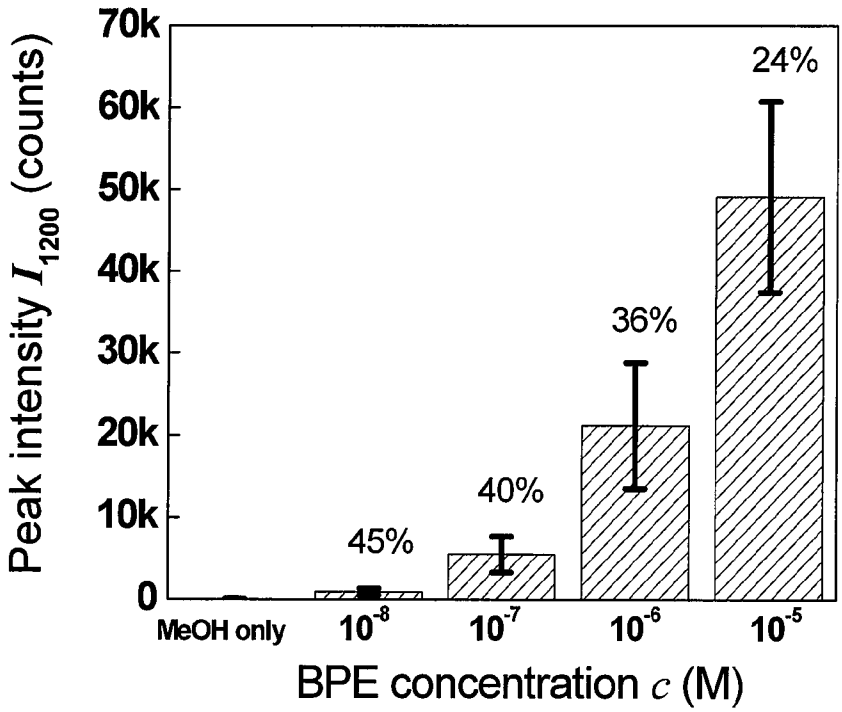
70k
60k
50k
40k
30k
20k
10k
0
Peak intensity I_{1200} (counts)
45%
40%
36%
24%
MeOH only
10^{-8}
10^{-7}
10^{-6}
10^{-5}
BPE concentration c (M)

FIG. 5G

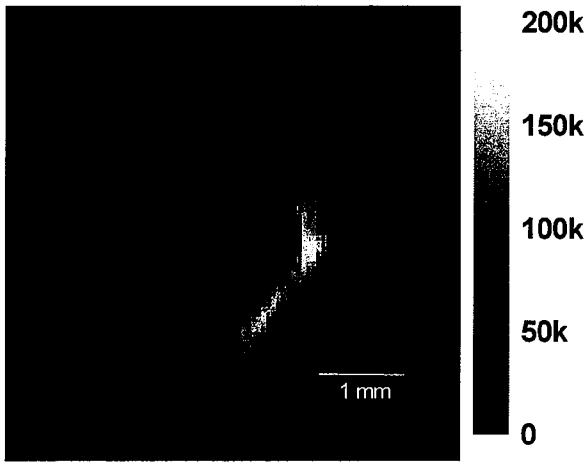

FIG. 5H

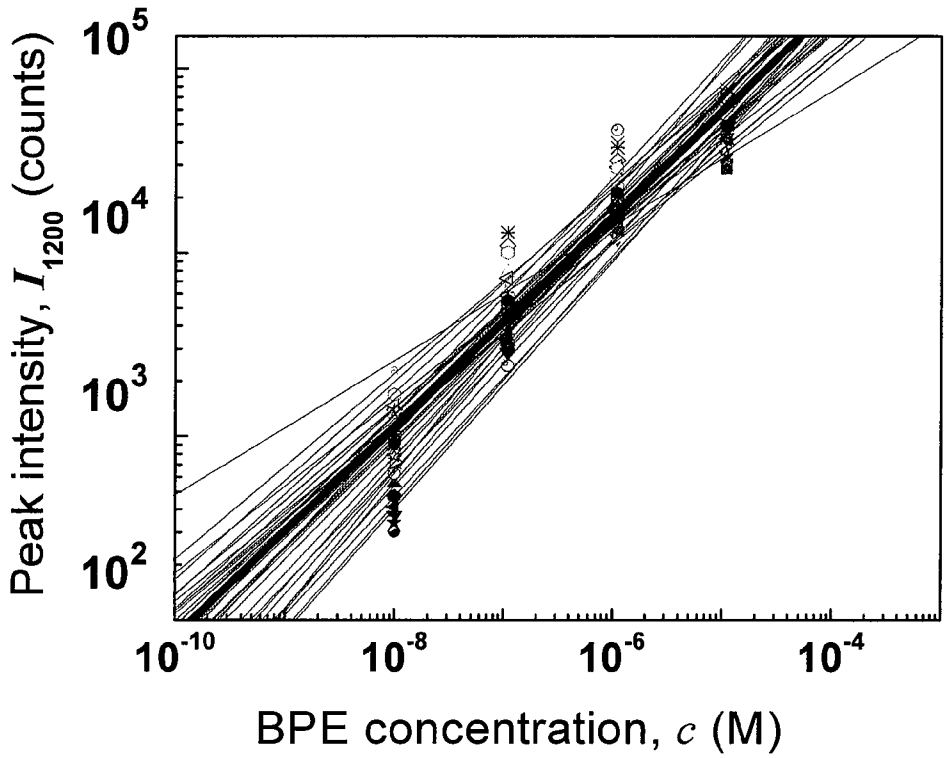
Peak intensity, I_{1200} (counts)
10^5
10^4
10^3
10^2
10^{-10}
10^{-8}
10^{-6}
10^{-4}
BPE concentration, c (M)

FIG. 6A

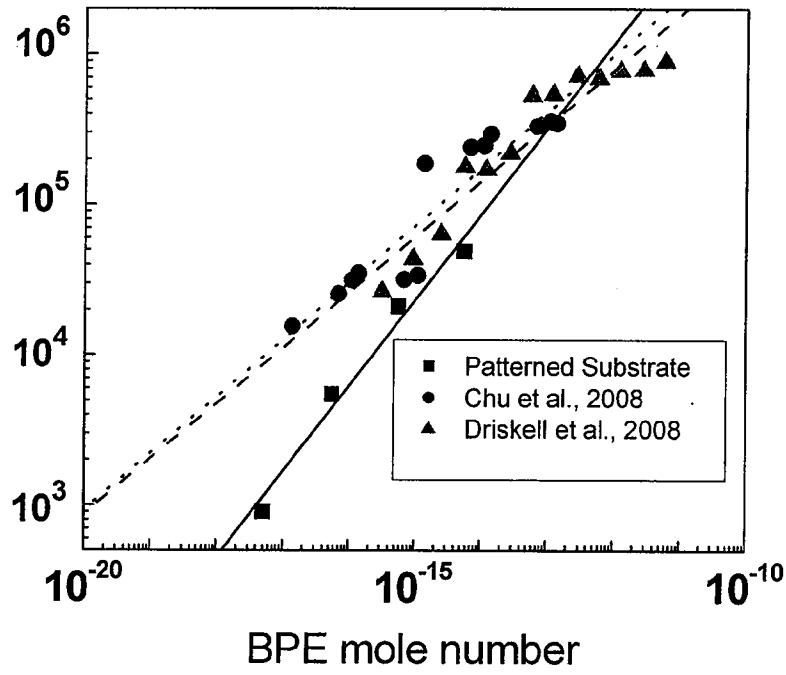
10^6
10^5
10^4
10^3
10^{-20}
10^{-15}
10^{-10}
Patterned Substrate
Chu et al., 2008
Driskell et al., 2008
BPE mole number

FIG. 6B

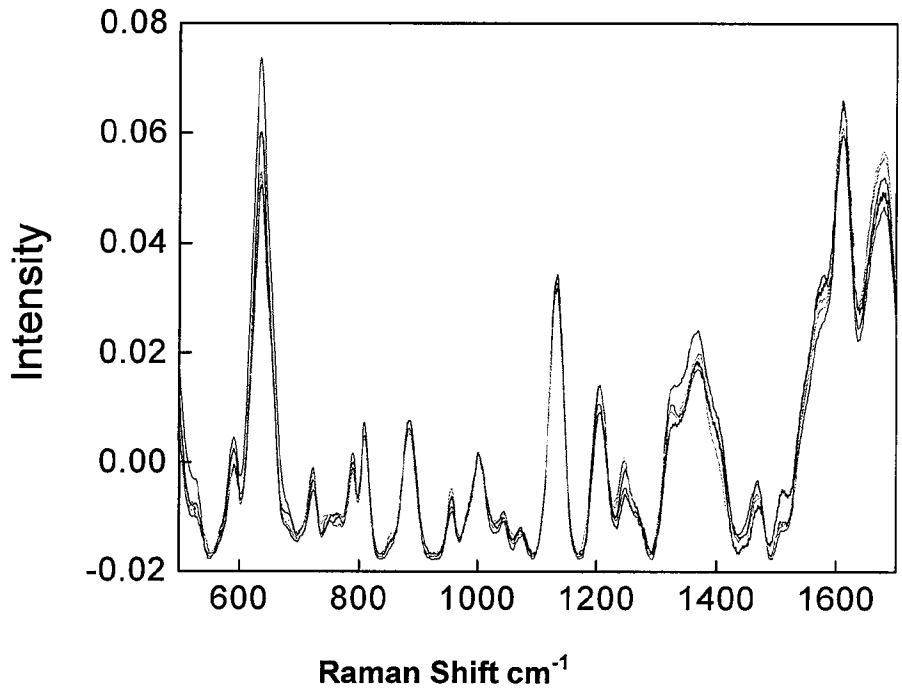
0.08
0.06
0.04
0.02
0.00
-0.02
Intensity
600
800
1000
1200
1400
1600
Raman Shift cm-1

FIG. 7A

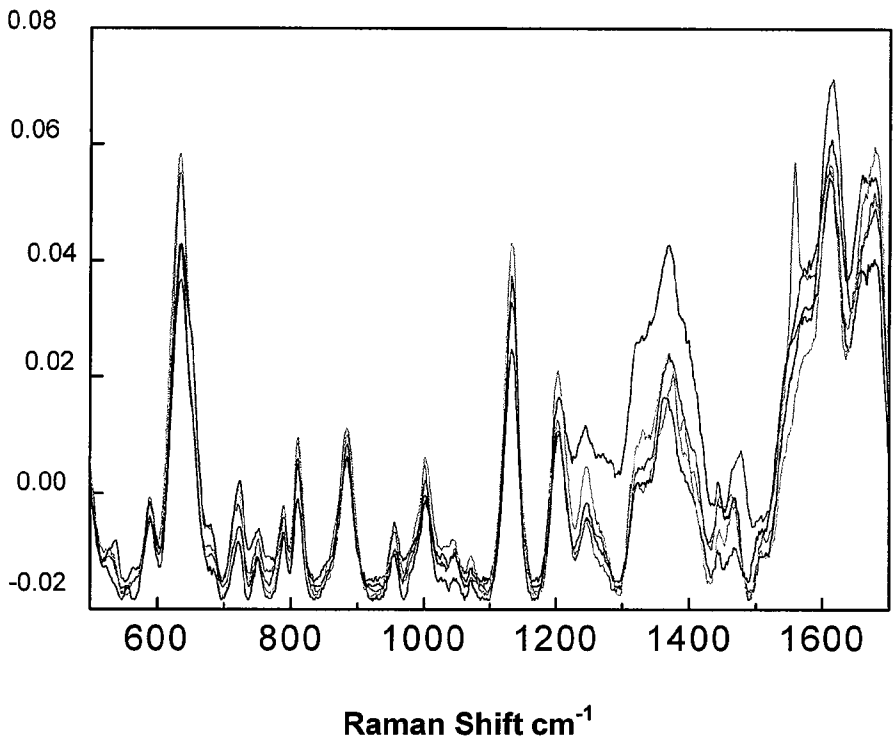
0.08
0.06
0.04
0.02
0.00
-0.02
600
800
1000
1200
1400
1600
Raman Shift cm-1

FIG. 7B

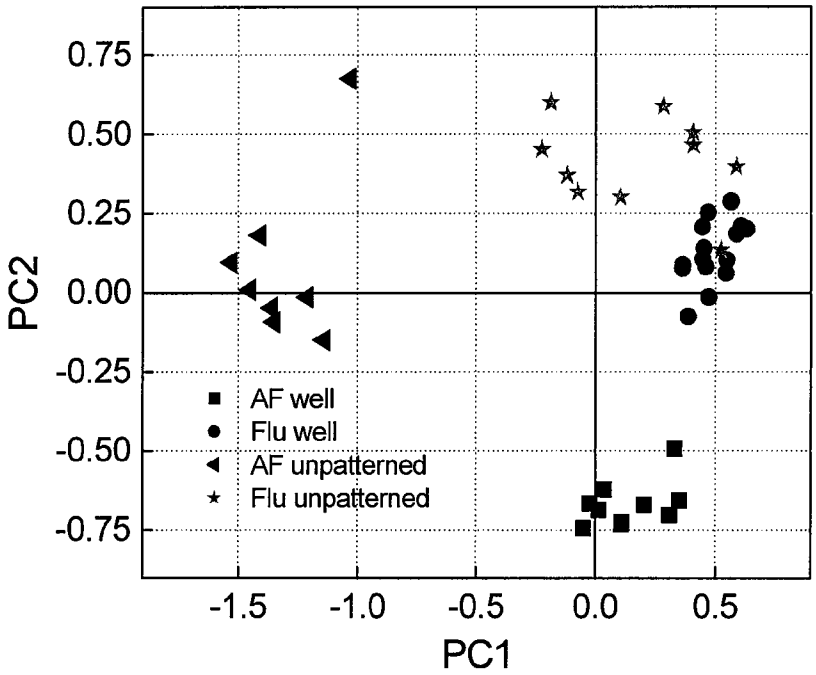
0.75
0.50
0.25
0.00
-0.25
-0.50
-0.75
PC2
-1.5
-1.0
-0.5
0.0
0.5
PC1
AF well
Flu well
AF unpatterned
Flu unpatterned

FIG. 7C

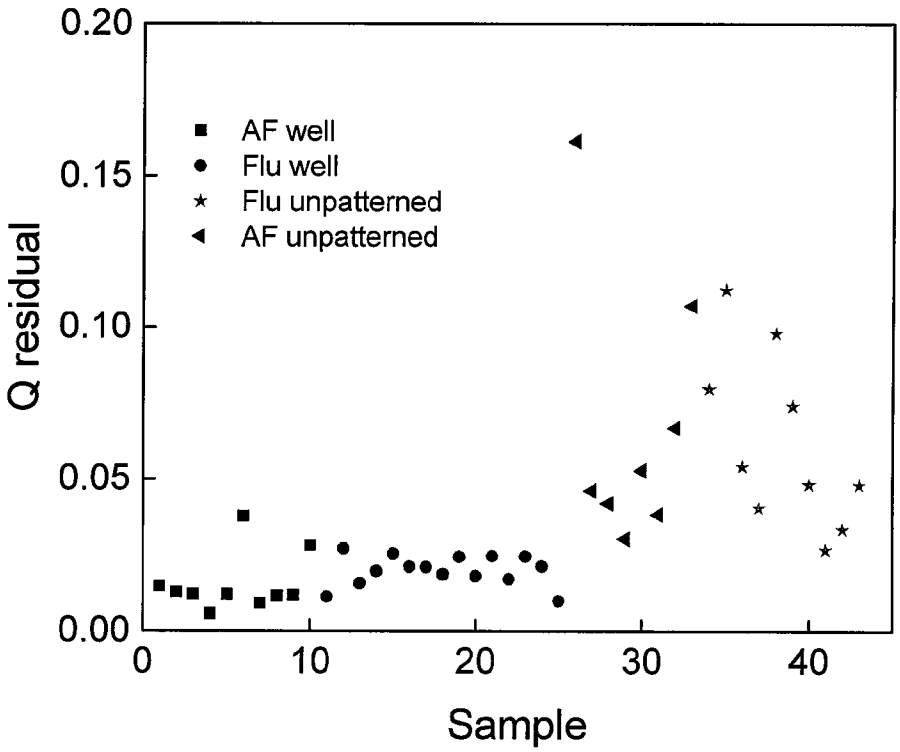
0.20
0.15
0.10
0.05
0.00
Q residual
0
10
20
30
40
Sample
AF well
Flu well
Flu unpatterned
AF unpatterned

FIG. 7D

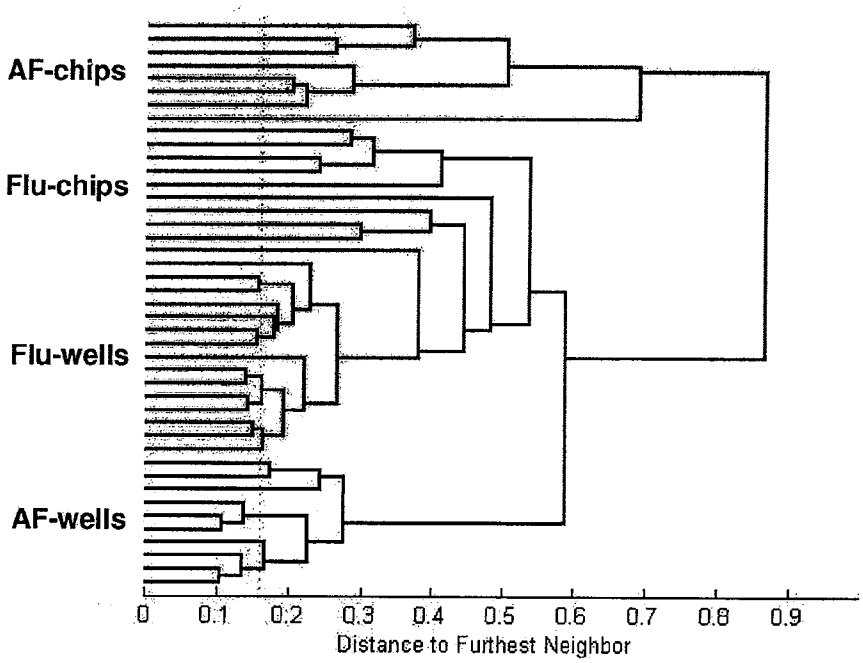
AF-chips
Flu-chips
Flu-wells
AF-wells
0
0.1
0.2
0.3
0.4
0.5
0.6
0.7
0.8
0.9
Distance to Furthest Neighbor

FIG. 8

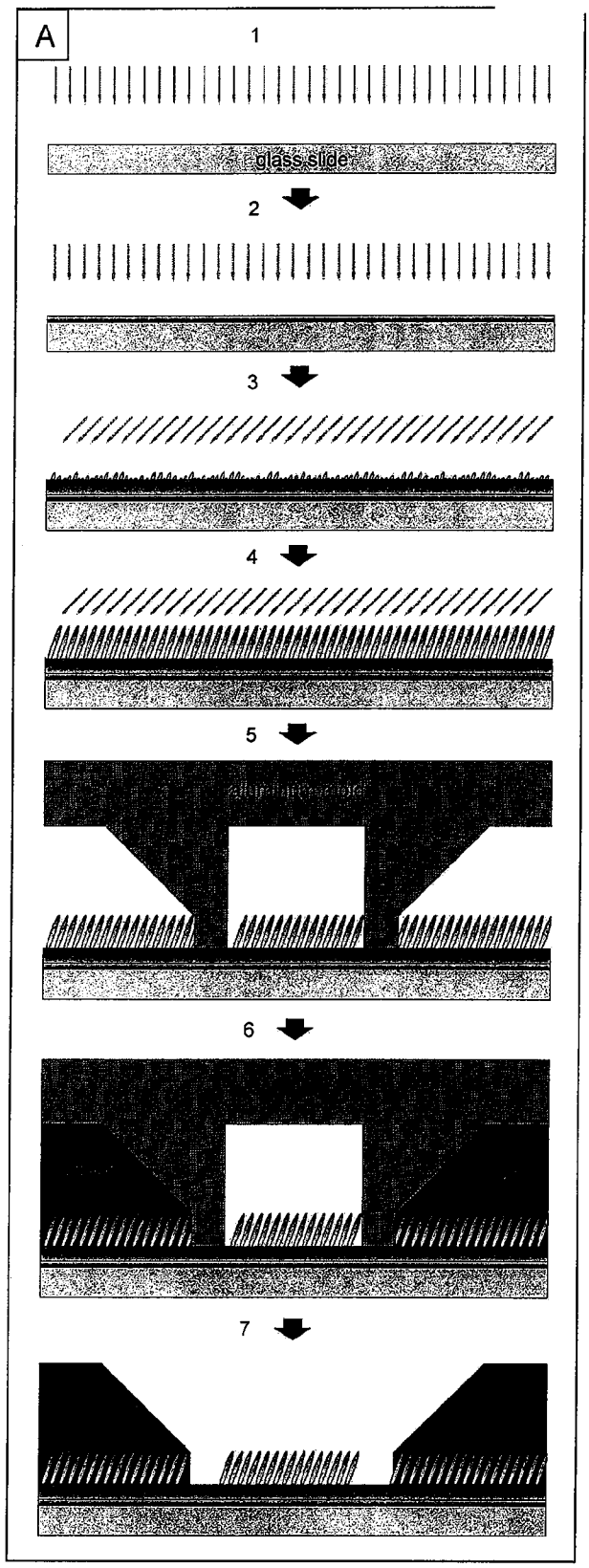

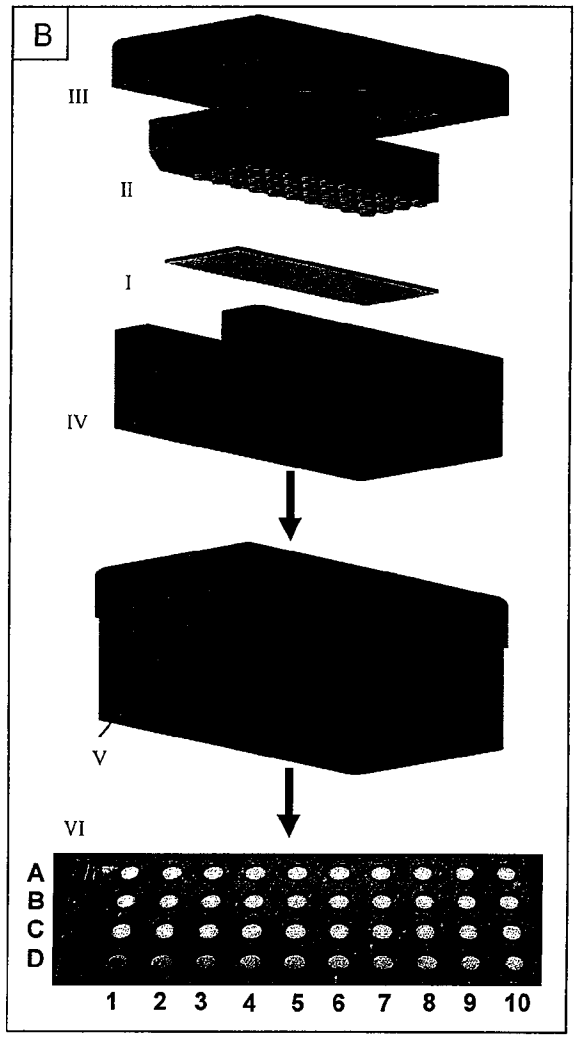

FIG. 9

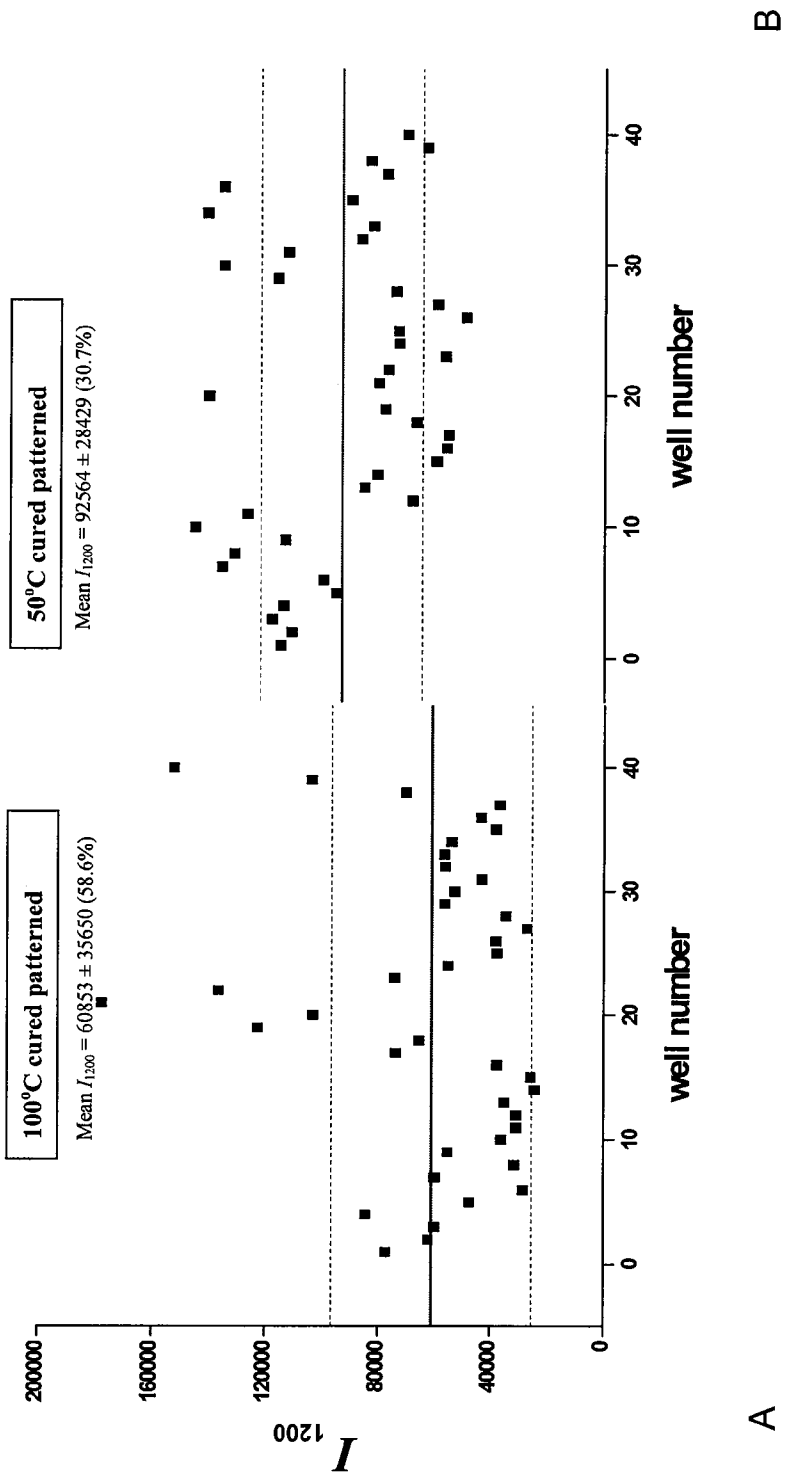
100°C cured patterned
Mean I_{1200} = 60853 ± 35650 (58.6%)
50°C cured patterned
Mean I_{1200} = 92564 ± 28429 (30.7%)
I_{1200}
200000
160000
120000
80000
40000
0
0
10
20
30
40
well number
well number
A
B

FIG. 10

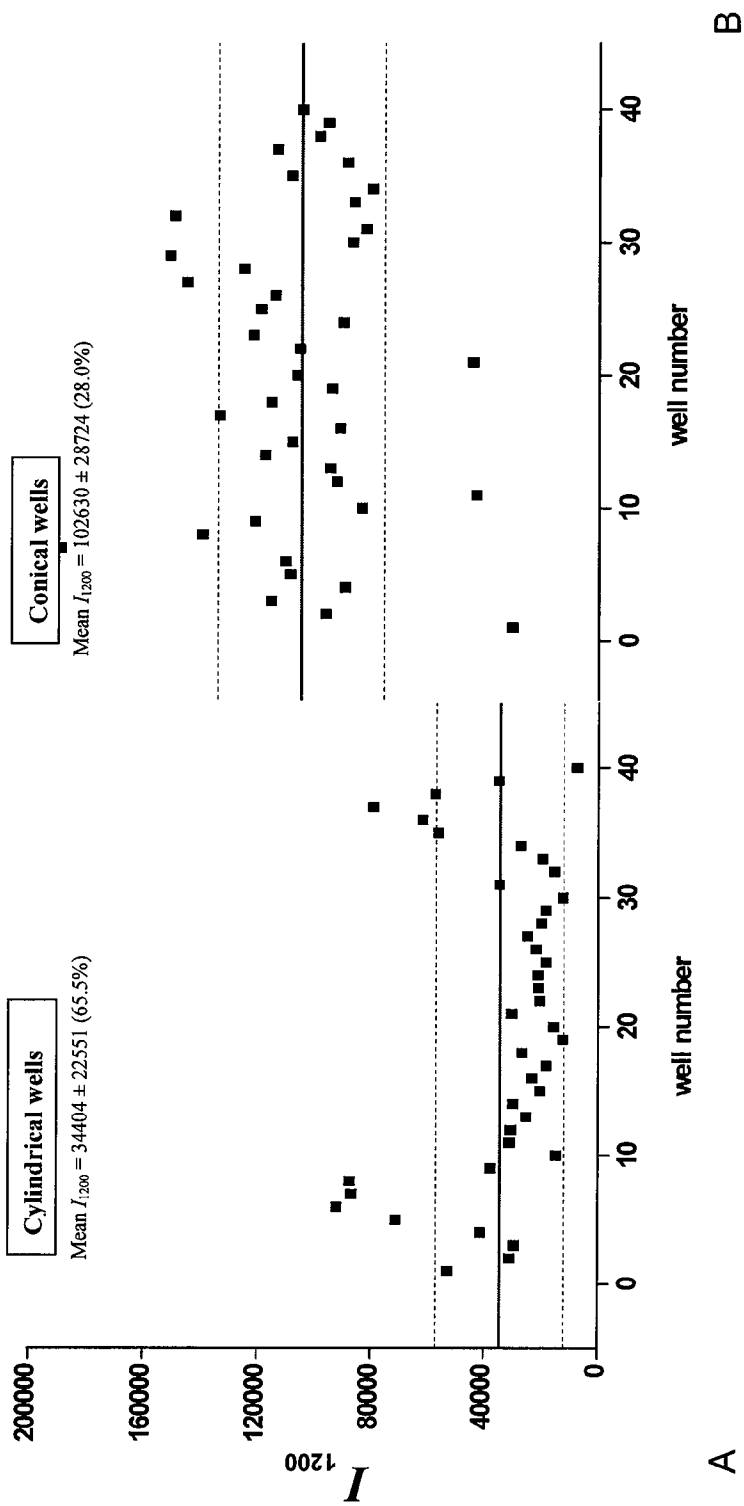
Cylindrical wells
Mean I_{1200} = 34404 ± 22551 (65.5%)
Conical wells
Mean I_{1200} = 102630 ± 28724 (28.0%)
I_{1200}
200000
160000
120000
80000
40000
0
0
10
20
30
40
well number
A
B

FIG. 11